Label-Free Sensing in Microdroplet-Based Microfluidic Systems

Ali Kalantarifard, Abtin Saateh [ID] and Caglar Elbuken *[ID]

Institute of Materials Science and Nanotechnology, National Nanotechnology Research Center (UNAM), Bilkent University, Ankara 06800, Turkey; a.kalantarifard@bilkent.edu.tr (A.K.); abtin.saateh@bilkent.edu.tr (A.S.)
* Correspondence: elbuken@unam.bilkent.edu.tr; Tel.: +90-312-290-3550

check for updates

Abstract: Droplet microfluidic systems have evolved as fluidic platforms that use much less sample volume and provide high throughput for biochemical analysis compared to conventional microfluidic devices. The variety of droplet fluidic applications triggered several detection techniques to be applied for analysis of droplets. In this review, we focus on label-free droplet detection techniques that were adapted to various droplet microfluidic platforms. We provide a classification of most commonly used droplet platform technologies. Then we discuss the examples of various label-free droplet detection schemes implemented for these platforms. While providing the research landscape for label-free droplet detection methods, we aim to highlight the strengths and shortcomings of each droplet platform so that a more targeted approach can be taken by researchers when selecting a droplet platform and a detection scheme for any given application.

Keywords: microdroplets; microfluidics; two-phase flow; digital microfluidics; label-free sensing

1. Introduction

The interest in the ability to manipulate fluids at small scale grew steadily leading to a variety of platform technologies. The initial methods in the field of microfluidics were mostly inherited from molecular analysis, microelectronics and microelectromechanical systems [1]. The microfabricated channels, valves, and pumps were soon brought together for ingenious applications. Although the advantages of these systems were apparent, such as the use of low sample volume, integration of different functionalities, higher sensitivity and fine control of heat and mass transport, they had fundamental limitations due to Taylor dispersion and poor mixing [2]. These limitations originated from the laminar flow as well as surface adsorption related losses and contamination. To overcome such shortcomings, excessive channel lengths and higher sample volumes were used. As an alternative to conventional microfluidic systems, droplet-based techniques have been developed to boost the key benefits of microfluidics such as low same volume and ability to perform assays rapidly [3].

Droplet-based microfluidic devices rely on the use of individual fluid compartments, i.e., microdroplets, rather than a continuous fluid stream. The volume of the droplets varies extensively from microliters down to femtoliters. The fact that volume scales to the third power of length leads to remarkably small sample volumes that can still be finely controlled by structures at the microscale [4]. It is to note that a 1 μm diameter spherical droplet has a volume less than 1 fL. The decrease in the working volume attracted the researchers at the early years [3]. As droplet generation technologies have matured, the ability to generate monodisperse droplets at high throughput turned out to be another distinguishing feature of droplet systems. Encapsulation of biological materials such as nucleic acids, proteins, virus, single cells, into individual droplets paved the way to study large populations and collect a vast amount of data for statistical analysis [5]. Together with the ability to manipulate

droplets by merging, splitting, sorting, restoring and incubating them, the researchers devised a plethora of droplet systems with several interesting features that combine these basic operations for the application of interest [4].

Almost three decades after its birth, droplet microfluidic systems are at a transition point from singular proof-of-concept examples to integrated systems for real-life applications. The long-lasting quest for a killer application for droplet microfluidic systems resulted in droplet digital polymerase chain reaction (ddPCR) devices that surpass the conventional real-time PCR devices (qPCR) for precise copy number identification without using any reference curves [3,6,7]. Droplet digital PCR turned out to be especially critical for detection of rare targets and next-generation sequencing library quantification.

An awareness of the available sensing methods for droplet-based assays can open new avenues for biochemical applications of droplets. The end-point detection is usually the component that limits the droplet-based system in terms of droplet frequency (throughput) and volume of analysis [8]. Therefore, a thorough understanding of droplet sensing technologies is required when designing a droplet-based assay. In this review, we aim to provide an overlook of label-free techniques that are used for sensing of droplets. As can be seen from the exemplary systems covered in this article, droplet microfluidic platforms blur the boundaries between the fundamental disciplines of science (physics, biology, and chemistry), requiring a more trans-disciplinary approach when designing new systems. Therefore, in this review, instead of classifying the literature in terms of applications, we prefer to lay out the basic droplet sensing tools that can be integrated for any given need.

There are numerous reviews on droplet-based microfluidic systems focusing on droplet generation [9–11], droplet manipulation [12–14] and applications such as single cell analysis [15,16], biochemical detection [17] and synthetic biology [18]. Specifically, this review aims to summarize the label-free sensing systems demonstrated using microdroplets. We first describe the main four droplet platforms and their distinguishing characteristics. The emulsion-based droplet generation methods have been omitted intentionally to focus primarily on more recently developed droplet microfluidic technologies. Then, we discuss label-free microdroplet sensing methods by listing some of the seminal work in each category. Finally, we give a brief comparison of these techniques and provide an outlook for future studies.

2. Microdroplet Sensing Platforms

This section discusses different types of droplet-based systems. We classify the droplet microfluidic systems into four categories: dispensed (or printed) droplet systems, segmented droplet systems, digital droplet systems, and slip-chip devices. Schematic representation of these systems is given in Figure 1. As seen from this figure dispensed droplet (Figure 1a) and slip-chip (Figure 1b) devices provide stationary droplets, whereas digital (Figure 1c) and segmented (Figure 1d) microfluidic systems study moving droplets. Another distinction can be drawn regarding the throughput. Dispensed and digital microfluidic droplet systems are suitable for low-throughput applications, whereas slip-chip and segmented droplet systems can be preferred for high-throughput uses.
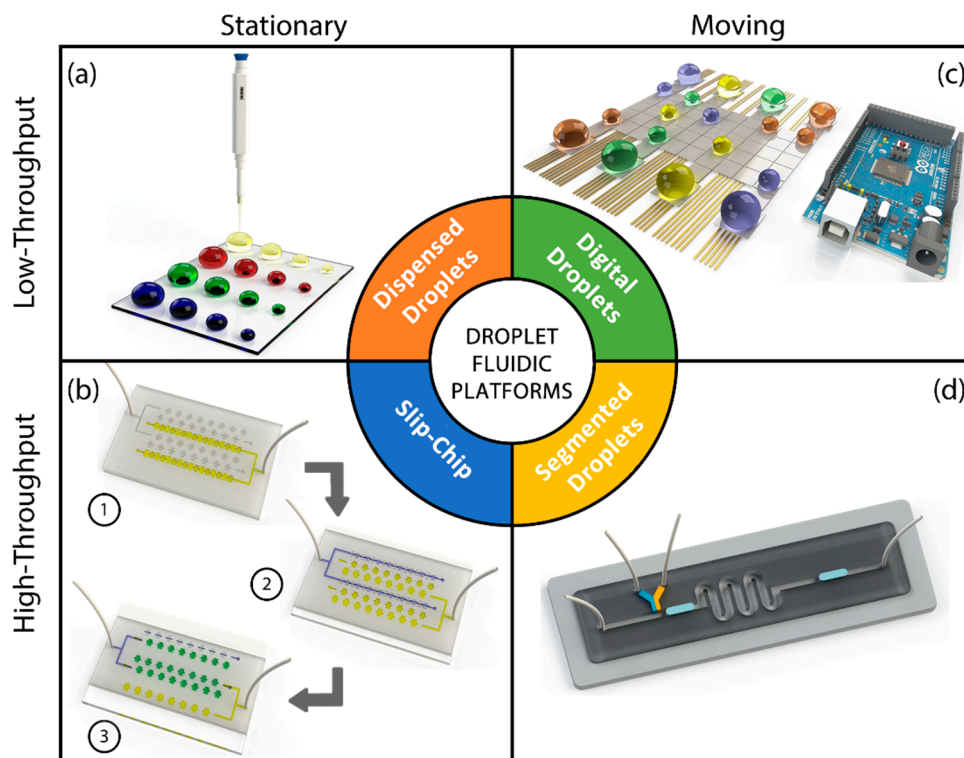
Figure 1. Various microfluidic droplet platforms: (**a**) dispensed droplets; (**b**) slip-chip; (**c**) digital droplets; (**d**) segmented flow droplets.

2.1. Dispensed Droplet System

In dispensed droplet systems, microdroplets of sample solution are deposited on a substrate in a well-ordered manner creating a planar array of droplets (Figure 1a) [19]. In these platforms, the droplets are static and do not contact each other. These systems are equivalent to well-plate assays with the exception that well size and number of wells can be reconfigured by the dispenser settings. Dispensed droplet systems can be regarded as virtual well-plate systems. These systems are handy when immobility of the encapsulated material is a requirement. In addition, as opposed to the moving droplet systems, dispensed droplet platforms provide easy indexing of droplets that might be critical when a combinatorial analysis is performed. Although evaporation is a major concern for such systems, it can also be turned into a benefit. Controlled gradual evaporation of the deposited droplets yields an increase in analyte concentration that allows analysis of the encapsulated material inside droplets for obtaining variation in concentration, interaction kinetics, conductivity and osmotic pressure [20–26].

Another major property of dispensed droplets is being immobilized and stationary on a surface. For heterogonous droplets, this would lead to sedimentation-induced reaction kinetics that might be of interest for some applications [19]. Also, if droplets are immobilized on patterned surfaces, they can be used for analysis of droplet content in certain orientations and patterns. For most dispensed droplet systems the substrate does not contain any sensors and detection is performed using non-contact methods, camera-based imaging being the most common one [27].

2.2. Slip-Chip System

SlipChip platforms have recently emerged as high throughput microfluidic systems that are favorable for their simplicity and multiplicity in performing simultaneous reactions without the use of peripheral components such as flow/pressure sources or valves [28]. A standard SlipChip device is composed of two patterned plates, a top plate with separated wells and another plate with channels and wells (Figure 1b). The main strength of a SlipChip platform is the increased throughput and the

ability to merge and split all droplet reaction chambers simultaneously. This feature allows researchers to operate reactions between a sample and different reagents individually and simultaneously which is critical for some applications such as protein crystallization. A SlipChip assay is usually performed in three steps: supplying reagents, supplying a sample and sliding the plates. Preloading wells with various reagents and filling patterned channels with a sample allows having reactions of various reagents with the same sample at constant mixing and reaction time just by sliding the top plate over the bottom one. Additionally, portability and ease of fabrication have turned SlipChip platforms to be attractive alternatives for chemical reaction analysis.

2.3. Digital Droplet System

A digital droplet platform is a droplet platform which is based on electrowetting-on-dielectric (EWOD) effect. EWOD makes it possible to manipulate individual droplets on a substrate by changing droplet contact angle with the application of a potential difference (Figure 1c) [29]. Applying AC or DC voltage to electrodes results in variation of interfacial tension that causes a change in wettability and, therefore, moves the droplet through virtual channels that are defined by sequential activation and deactivation of electrodes patterned on the substrate. AC voltage is preferred over DC to prevent insulator charging which leads to enhanced positioning accuracy of the system. Based on the configuration of the integrated electrodes, EWOD platforms are categorized into two groups: open and closed platforms [29]. In the open platforms, all the electrodes (actuation and ground electrodes) are at the bottom surface of the device and microchannels are exposed to the air. In the closed platforms, ground and actuation electrodes are integrated at the top and bottom surfaces, respectively. Using oil as a carrier fluid in closed platforms helps to ease the droplet motion and minimize evaporation that leads to automated droplet manipulation for extended assay durations. Using electrically controlled digital droplet platforms, researchers can manipulate droplets precisely and carry out various operations without using flow sources or additional components such as pumps and valves. Moreover, thanks to integrated microelectrode arrays, digital droplet platforms are favorable to incorporate detection methods that require grid based positioning such as matrix-assisted laser desorption/ionization (MALDI) mass spectroscopy and surface plasmon resonance imaging (SPRi) [29].

2.4. Segmented Flow Droplet Systems

Segmented flow platforms are the most preferred droplet-based systems which are based on compartmentalization of one fluid (dispersed phase) within another fluid (continuous phase) inside microchannels (Figure 1d) [30]. Microdroplets are formed inside microchannels sequentially using different geometries [9]. The size of droplets and frequency of droplet generation can be modulated by channel geometry and tailoring the flow regime (squeezing, dripping and jetting). The presence of a microchannel provides these systems an exquisite control on droplet positioning that is used for multiple droplet operations such as droplet transporting, merging, splitting and mixing. Due to the availability of a wide range of basic droplet operations, segmented flow droplet platforms are widely utilized for a vast variety of applications.

The classification provided in this section is intended to facilitate the comparison of various droplet-based microfluidic systems. It should be noted that some systems may combine these techniques on a single device. An example of such a hybrid system was demonstrated by Cole and Abate et al. where they combined a segmented flow droplet system with a dispensed droplet platform to obtain a system that can be used for single cell studies on a planar array that has the ability to immobilize specific cells in predetermined locations on a substrate [31]. The system uses segmented droplet sorting and dielectrophoresis-enhanced printing to achieve higher throughput of programmable droplet positioning.

3. Label-Free Sensing Methodologies for Droplet Systems

While optical detection techniques are unarguably the most commonly used method for sensing applications in droplets, these techniques mostly rely on fluorescent labeling due to high sensitivity, the ability for multiplexed analysis and real-time detection matching the MHz range droplet generation schemes [32]. In addition to the well-known shortcomings of labeling (need for additional steps, higher cost, and invasiveness), the droplet platforms pose further challenges such as stability of fluorophores and their interaction with the surfactants which are usually absent in continuous flow systems. Such material incompatibilities may limit the use of optical detection for label-free droplet sensing. To resolve these issues, electrical detection and mass spectroscopy can be good alternatives. Additionally, some advanced characterization techniques can also be used for detection inside microdroplets [32]. These techniques are summarized in Figure 2. For the rest of this article, details of each of these techniques are given together with representative articles. The aim here is to lay out the available label-free droplet detection methods that are suitable for various droplet microfluidic platforms.
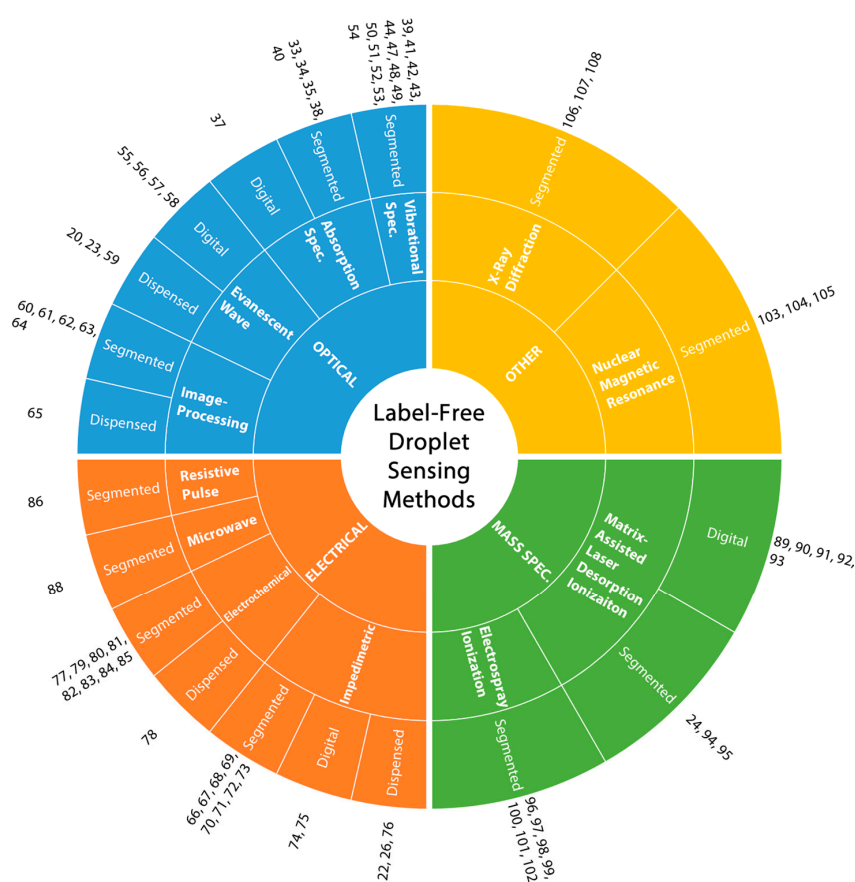

Figure 2. Classification of label-free droplet sensing methods. The main droplet sensing methods (optical, electrical, mass spectroscopy and other) are listed at the inner circle, followed by sub-classes and droplet platforms used for those sub-classes.

4. Optical Sensing of Droplets

Label-free optical detection of droplets can be grouped into four categories as schematically shown in Figure 3, absorption spectroscopy, vibrational spectroscopy, evanescent field sensing and image processing-based sensing. A major benefit of optical detection of droplets is that it is a non-contact measurement technique and it requires minimal changes to the fluidic system. Therefore, optical detection techniques can be applied to any platform, relatively easily.
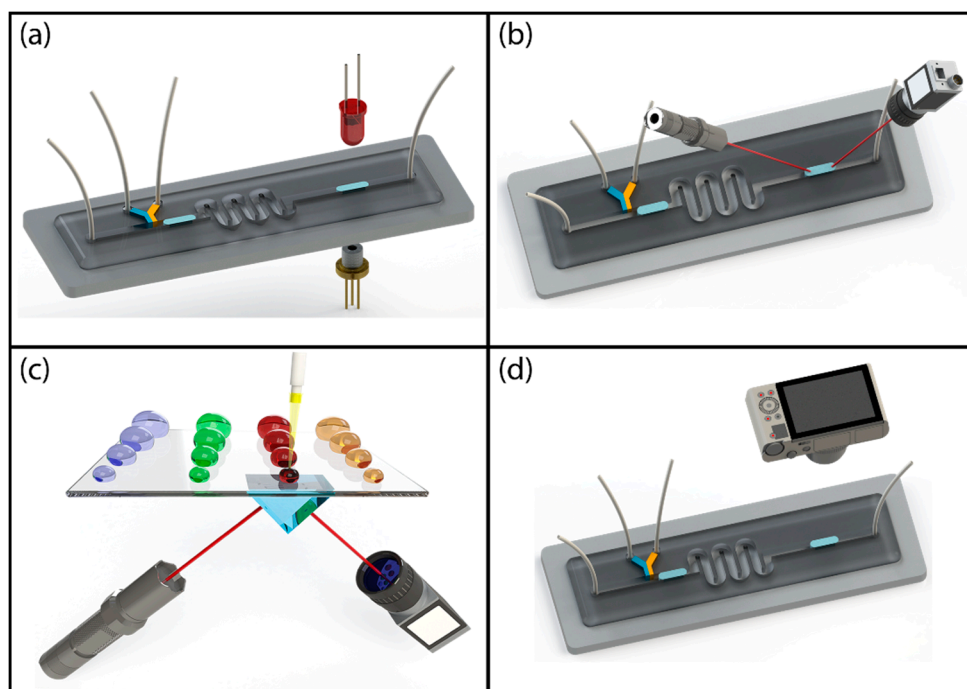
Figure 3. Schematic illustration of label-free optical detection techniques: (**a**) absorption spectroscopy; (**b**) vibrational spectroscopy; (**c**) evanescent field sensing; (**d**) image processing-based sensing.

4.1. Absorption Spectroscopy

For optical characterization of solutions, absorption spectroscopy is one of the most fundamental analytical methods (Figure 3a), although its application to microscale droplet-based studies has been limited fundamentally due to the small optical path lengths and poor sensitivities. Neil and Mackenzie et al. have addressed this issue by using multiple reflections in an optical cavity formed by two highly reflective mirrors [33]. They achieved a broadband detection system with relatively high detection speed. As opposed to simplistic optical detection techniques, they provide spectral absorption in the whole visible spectrum for characterization of multiple analytes inside droplets with high temporal and spatial resolution.

An alternative technique to address the optical path length problem is to integrate the optics horizontally in-line with the microchannel structure and get the incident light to interact with the sample through the channel width which can be made higher than the channel height. In this way, by simply increasing the width of the microchannels, sample absorption can be increased. Mao and Huang et al. have shown such a system, where they have integrated the optics with the microchannels using optical fibers [34]. They used two fibers that are coupled to the light source and the spectrophotometer. The reference absorption measurement was performed through the continuous phase section of the chip using oil absorption. They used an enzymatic reaction of a substrate molecule inside microdroplets to study reaction kinetics by changing the reaction time by adjusting droplet velocity inside the microchannel. They also studied the potency of an inhibitor molecule for the model reaction they have investigated.

An alternative technique is to collect the microdroplets in a cuvette and perform absorption spectroscopy as is done conventionally. Hung and Lee et al. have performed such a study, where they used a segmented flow system to study on-chip microdroplet merging and synthesis of CdS nanoparticles [35]. The microdroplets were collected at the outlet into a 10 mm path length quartz cuvette for absorption spectrophotometer analysis. The nanoparticles that were formed in the microfluidic device by droplet fusing and mixing showed better chemical stability with reduced aggregation compared to the ones formed by pre-mixed chemical solutions.

The roots of the droplet absorption spectroscopy measurements go back to the very first droplet studies, where optical absorption through droplets was utilized by a light emitting diode (LED) and a photodiode (PD) pair [36]. Srinivasan et al. have shown label-free optical characterization for determination of glucose concentration in bodily fluids such as blood, plasma, serum and urine for a digital droplet system [37]. They obtained a very good correlation between the reference method and the digital droplet platform except for urine sample which is attributed to the uric acid interference with the enzymatic reaction. The limited optical path length problem was addressed by having 500 μm gap between the two plates and using relatively large droplets with droplet volumes of 1.3 μL and 1.5 μL.

This simplistic optical absorption measurement can be scaled up using multiple LED-PD pairs for multipoint detection to study enzymatic reactions with high temporal resolution. Hassan, Nightingale, and Niu have demonstrated such a system based on segmented droplet system (Figure 4a) to study glucose oxidation reaction kinetics and measured the reaction rate using the Michaelis–Menten model [38]. They used seven sensors placed in a custom-made chip holder rig to obtain real-time information for segmented droplets that are transferred into a polytetrafluoroethylene tubing after formation. They used low-cost components to achieve a budget-friendly analysis system that can be potentially applied in the field.

4.2. Vibrational Spectroscopy

Vibrational spectroscopy is one of the most common methods used for label-free identification of molecules at a very low concentration based on their molecular vibration fingerprints (Figure 3b). It provides information about the molecular composition, structure, and interactions within a sample. There are two techniques used in vibrational spectroscopy: infra-red (IR) and Raman spectroscopy. In IR spectroscopy, change in dipole moment leads to a peak in the resultant spectrum when the sample is excited with IR light. The dipole moment changes when there is an antisymmetric vibration mode in the molecule. On the other hand, in Raman spectroscopy, the scattered light is probed which is mostly excited by visible light. Inelastic scattering of the light, in which case energy is transferred between photons and molecules, is the fundamental principle of Raman spectroscopy [39]. Raman spectrum of a molecule is a function of its polarizability change during molecular vibrations. The Raman signal varies based on the size, shape, and orientation of the electron cloud around a molecule. Unlike IR spectroscopy, the symmetric vibration which has more change in polarization is dominant in Raman measurements.

Integration of the vibrational spectroscopy to the microfluidic systems is critical when low concentration molecules are sought after. For the droplet-based systems, vibrational spectroscopy should be conducted in a way so that the aqueous medium does not affect the detected signal. Water molecules have low symmetric stretching leading to a low baseline signal for Raman spectroscopy, which makes it preferable for droplet fluidic systems in comparison to IR spectroscopy.

4.2.1. Infrared (IR) Spectroscopy

There are only a few studies that show infrared spectroscopic detection of droplets since most applications of droplets require aqueous samples for which water gives very strong signal suppressing the signal from the analyte. Chan and Kazarian et al. demonstrated the Fourier transform infrared spectroscopic (FTIR) measurement in a segmented droplet system for a region of interest of 2.5 mm × 2.5 mm [40]. They used a 64 × 64 focal plane array detector and obtained a scanning rate of 8 images/s. To demonstrate the capabilities of the system, first water droplets, then droplets with dilute lysozyme solutions were used. The droplets were formed inside a wax printed microfluidic channel. The system has limited temporal and spatial resolution. In order to improve the sensitivity of the system, Müller and Dietler et al. combined IR absorption with atomic force microscope (AFM) detection for an immobilized droplet array system [41]. The thermal expansion due to IR absorption was measured mechanically by an AFM cantilever achieving a nanoscale spatial resolution. This system uses a combination of segmented flow droplet generation and droplet printing techniques

to immobilize the droplets on a planar substrate for simultaneous IR radiation. In order to place the droplets as an array on the surface, the droplet solution was stamped by a patterned polymer slab which contains arrayed wells. Each well captured individual droplets so that droplets were placed with uniform spacing on the detection surface. Droplets were dried, and the monomeric and aggregated lysozyme content of the droplets were measured using this thermomechanical method.

4.2.2. Raman Spectroscopy

Raman spectroscopic detection of droplets is much more common due to the molecular fingerprint Raman measurements provide for aqueous samples. Barnes and Beers et al. performed one of the initial examples of Raman spectroscopy on segmented droplet systems [42]. They detected a photopolymerization reaction inside an aqueous continuous phase. Thanks to the low Raman response from the aqueous-phase, they were able to quantify the droplet composition for a photopolymerization reaction. For the detection system, they used a fiber optic Raman probe in backscattering mode with a focused beam diameter of 200 μm to probe individual droplets. Due to low Raman signal, a single spectrum was obtained every 3 min.

Cristobal and Servant et al. showed the application of Raman spectroscopy for droplet systems [43]. As an example, they showed the quantitative measurement of fluid mixing inside segmented microdroplets using standard PDMS microfluidic channels. They collected the Raman spectrum in 10 s by averaging signals over 750 droplets and the continuous phase fluid separating the fluids. They used aqueous solutions of $K_4Fe(CN)_6$ and $K_3Fe(CN)_6$ which give strong Raman signals due to C≡N stretching bond. The Raman signal is a function of the ratio of the length of the droplet to inter-droplet distance. Later on, the same group showed another work where they removed the background signal due to the continuous phase and the bulk PDMS chip [44]. They performed Raman measurements on a mixing reaction to compare the continuous flow mixing and segmented flow mixing. In this study they used H_2O and D_2O solutions which yield a rapid isotopic exchange reaction when mixed. They reduced the spectrum acquisition time down to 5 s and obtained results averaged over approximately 900 droplets. Their results clearly show the efficient mixing of two aqueous solutions inside moving droplets as the droplet is going through bending channels, which is known to generate stretching and folding vortices inside the microdroplet [45]. This hydrodynamic effect significantly increases the contact area between the fluids entrapped inside the microdroplet.

These initial studies of Raman spectroscopy droplet sensing used time-averaging to improve the signal to noise ratio for the low Raman signal amplitude. A major improvement in Raman sensitivity can be achieved by using surface-enhanced Raman spectroscopy (SERS) using the plasmonic effect of metallic surfaces. Placing the analyte in the vicinity of a nanostructured metallic surface excited by the visible light helps to enhance the detected scattering signals [46].

Jürgen Popp's group has demonstrated the very first few examples of SERS detection using segmented droplet microfluidic systems. Their main motivation was to prevent the surface adsorption of analyte/nanoparticle complex and also obtain a consistent SERS signal using minute amounts of analyte. The benefit of droplet systems over the conventional single phase continuous microfluidic systems is the fact that the analyte and metal nanoparticles are confined inside droplets and they do not interact with the channel walls. Thus, the non-specific adsorption to the channel walls and the spatial distribution of signal change were eliminated using well-mixed droplets. Moving droplet systems, such as digital droplet and segmented droplet systems, are favorable for SERS optical detection. The continuous movement of the droplets results in a homogeneously mixed droplet content which resolves the issues of non-uniform SERS signals due to the heterogeneous particle distribution creating Raman hot-spots and gives out a consistent ensemble signal [47].

Strehle et al. showed a model experiment using a glass microfluidic chip which showed the SERS detection of crystal violet with the presence of gold nanoparticles [48]. Tetradecane was used as continuous phase and the elimination of memory effect due to confinement of the aqueous sample solution by the oil was proven. The Raman spectra were obtained in 1 s from individual droplets

of volumes changing between 60 nL and 180 nL. It is also important to note that glass channel microfabrication is more tedious compared to polymeric channel fabrication since it requires wet etching (using hydrofluoric acid in this case) followed by alignment and bonding of two symmetrical micromachined glass structures. However, once successfully fabricated, glass channels can be used for a variety of biochemical analyses.

Using the same platform with a slightly different channel design, Ackermann et al. showed SERS detection of varying concentrations of an antihistamine and tranquilizer drug, promethazine, and a cancer drug, mitoxantrone, inside segmented droplets over extended times [49]. The repetitive measurement of droplets with varying drug concentrations showed no cross-talk between droplets, demonstrating the strength of segmented flow for successive measurements.

Later on, the same microfluidic chip design was used for identification of nine strains of *E. coli* bacteria [50]. The colloid suspension is mixed with ultrasonically lysed bacterial solution, hence, the SERS spectrum carried information from all the cellular components. An extensive study has been performed by obtaining more than 600 spectra for each strain ending up in close to 6000 measurements to obtain a SERS library for *E. coli*. The database was later used for statistical identification of the given sample set. They have also demonstrated the time-efficiency of microfluidic segmented flow SERS measurements (1 s per spectra). The microfluidic device led to an order of magnitude improvement in terms of measurement time, which is very critical for statistical identification requiring a library of spectra. The highly controlled microenvironment together with the ability to average through a chunk of repetitive data led to high repeatability.

Wang and deMello et al. used surface-enhanced Raman spectroscopy for detection of trace amounts of mercury (II) in aqueous samples for water toxicity testing [51]. They used a segmented droplet system which continuously moves the droplets through the Raman detection zone. They mixed the sample solution with gold nanoparticles during droplet formation. They have obtained one order of magnitude improvement in sensitivity compared to fluorescent detection. The same system was also used to show SERS detection of trace amounts of paraquat, again for drinking water safety [52].

SERS allows orders of magnitude improvement in signal-to-noise ratio in comparison to conventional Raman measurement. When the excitation frequency matches the frequency of the electronic transition of the target molecule an additional enhancement is obtained which is referred to as surface-enhanced resonance Raman spectroscopy (SERRS). Cecchini and Edel et al. demonstrated very repeatable SERRS detection at high speeds where multiple spectra (more than 50) can be obtained from individual segmented droplets [53]. A custom-made detection system was used together with standard PDMS microfluidic chips and silver nanoparticles for Raman signal enhancement as shown in Figure 4b. For the additional resonance enhancement malachite green (MG) was used. Syme and Cooper et al. used SERRS to demonstrate real-time simultaneous detection of two SERRS species [54]. Crystal violet and Rhodamine 6G dyes were used as reporters in addition to silver nanoparticles. The concentrations of the two dyes were gradually modified using an automated pumping system. Each spectrum was obtained in 20 ms and the changing droplet concentration was proved using the amplitude change in the two characteristic peaks in the successive SERRS signals. Such a system proves the ability of segmented droplet systems to be used for SERRS active target identification using internal standardization as the second probe molecule in the droplets.

4.3. Evanescent Field Sensing

Evanescent field sensing is based on the measurement of the exponential decay of an electric field of the propagated light in the microfluidic devices which enables total internal reflection (Figure 3c). It is a nondestructive label-free sensing method for detection of media with varying refractive indices using optical detection systems or resonators such as surface plasmon resonance (SPR), guided-mode resonance filter (GMRF) and microring resonator. Evanescent waves generated at the surface decay exponentially in the tangential direction to the surface. Therefore, detection is limited to a thickness less than a few hundred nanometers in the proximity of the surface.

One of the earliest examples of droplet evanescent field sensing was demonstrated by Valentino, Troian, and Wagner using a platform similar to digital droplet systems [23]. Microdroplets of 400 nL volume were dispensed on a planar surface with integrated thin-film waveguide. Droplets move across the optical detection region by changing the droplet contact angle by thermocapillary action using the embedded microheaters beneath the droplets. The system uses conventional optical components (prism couplers, He-Ne laser source, and photo-diode) and a high-end lock-in amplifier to detect the evanescent field attenuation due to surface interaction. As a model assay, droplets of various dye concentrations were studied, giving a logarithmic response to dye concentration. Reaction rate measurement as a function of surface temperature was also studied using this system.

Malic, Veres and Tabrizian applied surface plasmon resonance imaging (SPRi) for a digital droplet system [55,56]. SPR is commonly used to study surface binding interactions by probing refractive index change. Combining the multi-point detection of SPRi with the digital droplet system, they were able to monitor multiple droplets in the detection window. For this specific system, they did not use oil immersion and manipulated droplets using a closed digital droplet system, the top plate of which was modified to accommodate label-free SPR sensing. The evanescent field was generated by exposing 50-nm-thick gold layer to the sample. In addition to the common benefits of low sample volume and programmability, they also made us of the electric field actuation during DNA probe hybridization step. They showed DNA immobilization and DNA hybridization on gold-coated EWOD electrodes. By applying an electric field during surface functionalization step, the probe orientation and density were tuned resulting in higher DNA binding efficiency. This study demonstrates the potential of reconfigurable DNA array detection on a digital droplet platform.

Similarly, Arce and Bienstman et al. used a digital microdroplet platform for label-free evanescent field sensing using silicon microring resonators [57]. They placed twelve ring resonator sensors on the top plate of a digital droplet platform and performed refractive index change measurement to determine analyte concentration inside microdroplets. The incident laser was coupled to the chip with integrated gratings and resonance wavelength shift was measured at multiple sensors using an infrared camera. As a proof-of-concept experiment, they measured refractive index change due to the concentration change of sodium chloride, glucose, and ethanol inside the droplets.

Another example of a digital droplet platform for surface plasmon resonance detection was shown by Wang and Hsu et al. using a photonic crystal (guided mode resonance) [58]. The implementation of evanescent field sensing was implemented using a similar architecture. A parallel plate digital droplet system was used. Since the bottom plate is mostly populated with the electrodes for droplet motion, the three-layer optical sensor was implemented on the top plate. The detection performance of the system was evaluated using sucrose concentration measurements.

Wildgen and Dunn used whispering gallery mode resonance sensors excited by an evanescent field (Figure 4c). They used dispensed droplets of 10 µL volume [20]. The droplets are dispensed on the barium titanate resonators. The evanescently scattered light was measured using a microscope coupled to an avalanche photodiode. Since the droplets are exposed to air, evaporation is one of the major concerns for this configuration. Although evaporation can be beneficial to induce mixing inside the droplets and to improve material transport efficiency, it causes uncertainty for low concentration analyte detection due to dependence on environmental conditions. In control experiments, they demonstrated that setbacks due to sample evaporation can be eliminated by dipping the system in an oil bath, generating a liquid/liquid two-phase system with stationary droplets. Due to the impracticality of this approach, they performed their label-free measurements with droplets exposed to air and completed the measurements in the first few minutes after droplet dispensing when evaporation effects are minimal. They characterized the system by measuring salt concentration in droplets and finally demonstrated a model streptavidin/biotin binding rate measurement assay.

For dispensed droplet platforms, Yin and Tao et al. used surface plasmon resonance sensing using the common prism-coupling configuration [59]. A droplet of the solution of interest was pipetted on the resonance sensing surface and protein interaction kinetics were studied. Specifically,

association/dissociation rate constants and binding affinity were determined. They also compared the droplet-based approach to the conventional flow-through systems. As nicely reported, while dispensed droplet systems provide a reduction in the required sample volume, they may suffer from the evaporation effects and the lack of mixing for mass transport limited reactions due to the analyte-depleted region forming at the sensor surface.

4.4. Image Processing-Based Sensing

Combining droplet microfluidic systems with image processing is relatively easy since most microfluidic systems are tested or operated under a microscope (Figure 3d). Hence, having an image of the droplets does not require much expertise or budget since camera-attached microscopes are standard in most microfluidic laboratories. Additionally, thanks to the advancements of the imaging tools in consumer electronics industry, image processing can be performed much more easily using standard libraries. The only setback of image processing is that it only provides physical information about the droplets such as their size, shape, velocity or color. Therefore, for any sort of biochemical application of droplets, one of these features should be modulated so that image processing of droplets can be used for label-free sensing.

Glawdel, Elbuken, and Ren used image processing of high-speed camera recordings to understand the droplet generation dynamics for a T-junction channel geometry [60,61]. Using an automated setup, segmented microdroplets were formed in a microchannel using different combinations of continuous and aqueous phase solutions. The capillary number was changed while high-speed movies of droplet formation process were recorded. Then, analyzing these videos off-line using image processing algorithms, dispersed phase penetration depth, neck pinch-off thickness, droplet size, velocity, frequency and inter-droplet spacing were extracted. This study led to a thorough explanation of droplet formation dynamics and proposed a third-phase, named as lag-phase, during the continuous formation of microdroplets for T-junction microchannels in addition to the well-known two-phase model (filling and necking). This was a critical work to understand the droplet formation dynamics that is also essential for the formation of monodisperse droplets.

Later on, using a similar approach, A. Basu has developed an image processing tool for analysis of trains of droplets using video recordings [62]. This tool can be utilized to analyze the physical properties of droplets such as length, width, velocity, trajectory, spacing and shape deformation (Figure 4d). This technique does not require any fluorescent or dye-based tracer particles; instead, it relies on the contrast at the interfaces (fluid/fluid, fluid/solid interfaces) due to the refractive index difference. The software has built-in image processing functions such as background subtraction, edge detection, shape filling and shape identification (spatial information) as well as frame correlation for temporal analysis. It comes with a user-friendly interface and can be applied to a variety of applications. In the same study, the author demonstrated measurement of droplet generator, droplet splitting/merging analysis, evaluation of single cell encapsulation efficiency etc. This video processing-based technique can be used for all moving droplet systems. In order for it to be applicable to stationary droplet systems with full capacity, a video of the droplets can be obtained while moving the stage or the camera relative to one another. Using automated microscope stages or any type of motorized X-Y stage, this is a trivial task.

Zang and Roth et al. developed a real-time image processing-based system for label-free detection of picoliter volume droplets for high-throughput Actinobacteria culturing in a segmented flow system [63]. The droplets were analyzed optically, and empty droplets and microbial hyphae-laden droplets were identified. Downstream of the detection region, droplets were sorted using dielectrophoretic separation eliminating the empty droplets. This study demonstrates the strength of real-time image-processing without sacrificing the throughput of segmented flow droplet systems. For such applications, optimization of image processing algorithms is required to keep up with the high throughput performance of the fluidic system.

Hofmann and Böhm et al. used image processing as an indirect method to quantify the intra-droplet concentration changes due to metabolic activity of individual cells inside droplets [64]. They used the principle that size of individual droplets changes due to the transport of water between the continuous and dispersed phase induced by the osmotic pressure difference. The microdroplets containing yeast cells with YPD-medium shrunk in size when incubated. Hence, by monitoring the size of spherical microdroplets collected in a measurement chamber, they were able to determine the droplets containing viable cells. Additionally, analyzing the rate of change of droplet size, they reported the metabolic activity inside a specific droplet as an indicator of cell count and/or cell activity level.

Liao and Yeh demonstrated an interesting sensing mechanism based on contact angle change of dispensed microdroplets as a function of chemical content concentration [65]. Silicone oil solutions of differing bovine serum albumin (BSA) concentrations were prepared and dispensed on a gold-coated glass surface as droplets. A self-assembled monolayer (mercaptoundecanoic acid, 11-MUA) was formed on the glass surface. It has been shown that the contact angle of droplets increased with increasing BSA concentrations. The smaller the droplet size the more pronounced was the change in the contact angle. This principle can be extended to stationary droplet systems where an analyte may change the contact of the droplet, though such systems will have limited throughput since contact-angle measurements require more demanding side-view imaging.
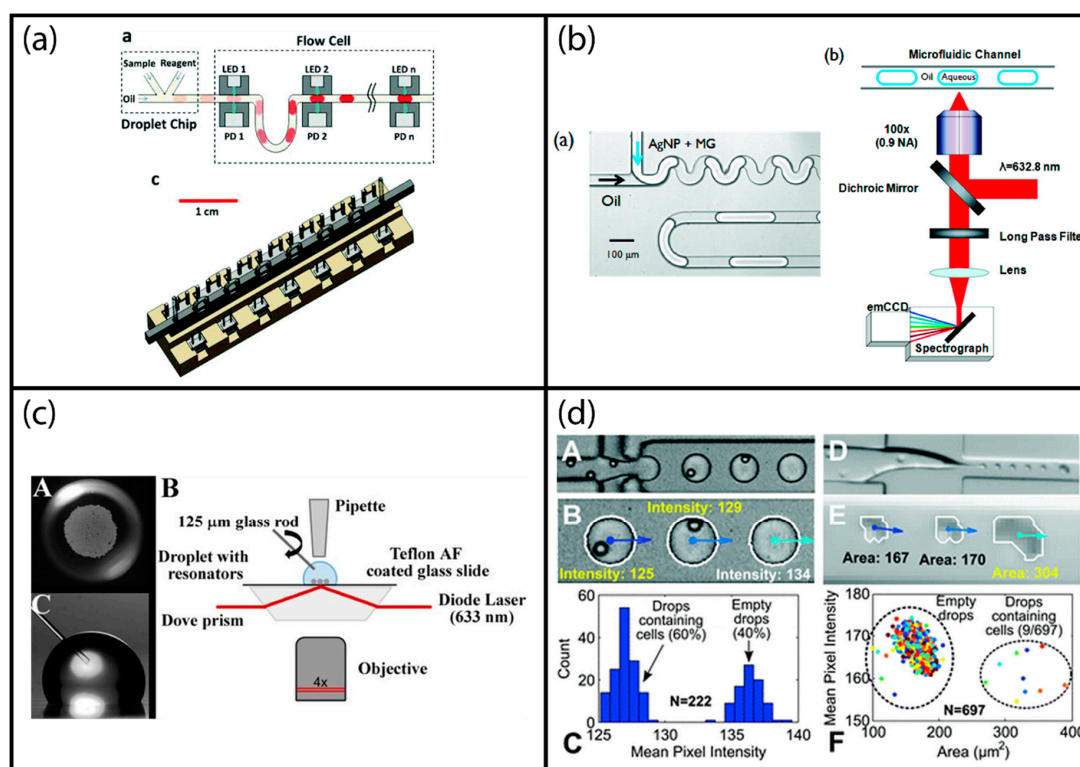

Figure 4. Examples of label-free optical droplet detection: (**a**) Multi-point optical absorption measurement of droplets moving inside a tubing; reproduced from [38] with permission of The Royal Society of Chemistry. (**b**) Surface enhanced resonance Raman spectroscopy (SERSS) detection adapted to segmented flow droplets using silver nanoparticles; adapted with permission from [53]. Copyright 2011 American Chemical Society. (**c**) Evanescent field sensing using whispering gallery mode resonance sensors; reprinted under Creative Commons Attribution License 4.0 from [20]. (**d**) Image processing-based sensing of segmented droplets; reproduced from [62] with permission of The Royal Society of Chemistry.

5. Electrical Sensing of Droplets

Another major domain of microdroplet detection techniques is electrical detection amongst which impedimetric (Figure 5a) and electrochemical (Figure 5b) detection are the most widely used methods. Electrical detection of droplets can be both contact and non-contact based. Analytical parameters such as limit of detection, sensitivity and dynamic range are primarily affected by signal-to-noise ratio and sampling rate, which depend on the detection instrument. Hence, it is difficult to give overarching values for the performance of electrical droplet sensing studies. Each work should be evaluated individually taking into account the specific type of electrical detection method used, the type of instrument and the choice of electrodes.
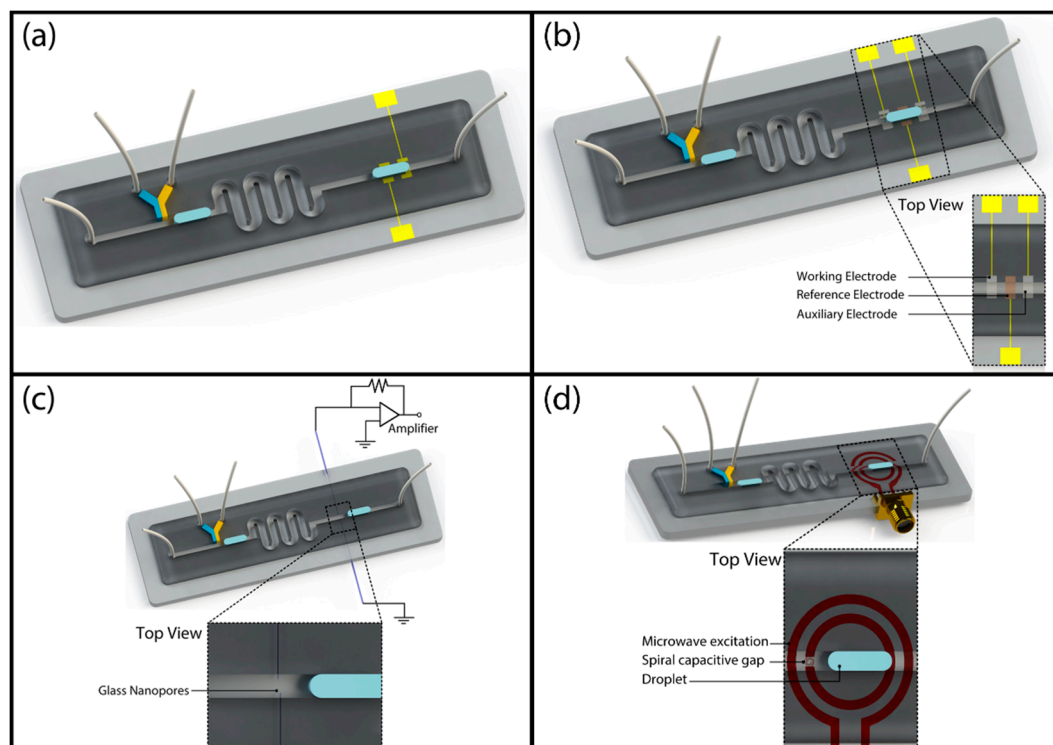

Figure 5. Schematic illustration of label-free electrical detection techniques: (**a**) impedimetric sensing; (**b**) electrochemical sensing; (**c**) resistive pulse sensing; (**d**) microwave sensing.

5.1. Impedimetric Sensing

Chen and Troian et al. performed one of the most fundamental studies for capacitive detection of microdroplets using a digital droplet system that uses thermocapillary droplet actuation [66]. They used coplanar electrodes for impedimetric sensing (Figure 5a) that are originally used as resistive heaters to generate the thermocapillary movement of the droplets for electrical sensing. They provided the analytical model for the semicircular electric field generated by coplanar thin film electrodes and verified it both numerically and experimentally. They also showed droplet sensing results for symmetric two-prong electrodes and interdigitated electrodes. They demonstrated preliminary results of sensing of droplet position, volume, and content setting the groundwork for the upcoming studies.

In order to increase the sensitivity, Srivastava and Burns used conductivity sensing with electrodes that are in contact with the solution [67]. In addition to detecting the presence of the electrodes, they placed the electrodes in the most common configuration which is fabricated underneath the microchannel and placed perpendicularly to the channel. They showed a second configuration where the two electrodes were placed parallel to the channel to detect the volume of the droplet by measuring the conductivity change between the two electrodes that are placed at the two sides of the microchannel.

Building on Chen's work, Elbuken and Ren et al. developed a high-sensitivity droplet capacitive system using off-the-shelf electronic components significantly reducing the cost and entry barrier for the implementation of capacitive detection [68]. They showed that droplet size and speed can be detected by using an electronic circuit that costs less than \$20. Additionally, the sensing unit was very small and can be applied to portable applications. Isgor and Elbuken et al. showed that using the same electrical circuitry droplet, content can also be measured [69]. The change in the dielectric content of the droplet, due to the mixing of ethanol and water at varying ratios, can be detected when a nanometer-thick SiO_2 layer is used as a passivation layer between the droplets and the planar electrodes.

Kemna and van den Berg et al. reported the impedimetric detection of viable single cells inside segmented droplets at moderate throughputs (112 Hz) [70]. They have modeled the system using lumped electric circuit models with an analogy to electrical circuits. The optimal frequency and electrical properties of materials can be determined by such a model. They showed that viable mouse myeloma cells present in water droplets yield a detectable signal using a high-end impedance spectrometer.

Simon and Lee et al. showed an interesting application of impedimetric detection by detecting polymerized DNA chains inside segmented droplets [71]. Using a microfluidic system and a detection circuitry similar to the previous study, they combined on-chip thermocycling to demonstrate the impedance signal difference between droplets with amplified and non-amplified DNA content. Although, the measurement is susceptive to slight changes in droplet size, once perfected it can be used for digital droplet PCR to alleviate the need for the fluorescent tagging [72].

Marcali and Elbuken showed impedimetric detection of hemagglutination inside segmented microdroplets [73]. As a model assay, they used blood typing to form agglutination positive and negative droplets using a microfluidic chip as schematically shown in Figure 6a. Using narrow electrodes placed perpendicular to the microchannel, they created a minimized detection zone to obtain a steady-state reading from droplets. Using the impedance data, they were able to differentiate between droplets of different content as well as droplets with agglutinated red blood cells.

Impedimetric droplet sensing was implemented on other droplet fluidic platforms, as well. Digital droplet systems already integrate coplanar electrodes with fluidics; hence, such an implementation is relatively easy for these systems due to minimal hardware changes required. Sadeghi and van Dam et al. modified a digital droplet system by simply adding a resistor to the AC actuation circuitry [74]. They showed that they can detect droplet volume, droplet type (DMSO or water) and droplet content (concentration of potassium fluoride) without sacrificing the droplet actuation and droplet handing performance of the digital droplet platform. Shih and Wheeler et al. showed the very first implementation of detection of mammalian cells inside droplets on a digital droplet system [75]. Instead of turning all actuation cells into sensors, they placed dedicated detection electrodes in between the actuation electrodes. Also, in order to obtain a statistically significant data to distinguish droplets with varying cell concentrations, they used a buffer exchange method. Just before the impedimetric analysis, they changed the cell buffer solution inside the droplet with low conductivity solution that was replaced by the original solution after the measurement.

Ernst et al. showed an integrated capacitive droplet measurement system for a dispensing droplet platform [76]. The sensor was very well integrated into the print head. Sensing of droplet volume was achieved by 3D electrodes that are placed through a custom designed printed circuit board (PCB). The electronics are also placed on the same PCB minimizing the signal loss due to electrical contacts. The fabrication of the sensor was achieved with a little tweak to the standard PCB fabrication process. The droplets were dispensed through a via which is used for inter-layer connections in PCB designs. After PCB fabrication, the via is sliced into two, forming symmetrical semi-cylindrical electrodes creating an axially symmetric 3D electric field. The droplets were dispensed through the center of the via and real-time droplet measurement was achieved. The system was not tested for any analyte sensing. It was mostly designed for droplet size control for bioprinting applications, but conceptually it can be applied to detect the content of droplets as well.

Impedance detection of droplets was also implemented on stationary droplets on a dispensed droplet detection system. Ebrahimi and Alam et al. showed a system which is composed of an array of nanostructured hydrophobically coated electrodes [22]. The sample was dispensed on the electrodes and real-time impedance measurement was obtained from stationary droplets. A very nice feature of this work was that they utilized the concept of evaporation induced concentration increase. Evaporation of droplets causes a decrease in droplet volume that in turn increases the analyte concentration beating the diffusion transport limit. The evaporation time was around 20 min when 3 μL droplets were used; 850 bp synthetic DNA fragments were used for the experiments. Using a lumped circuit model, they modeled the electrical circuit interpretation of DNA concentration increase during the experiment. They showed that using evaporation induced sample enrichment, an order of magnitude improvement can be obtained in the limit of detection. This enrichment concept has been applied to many other systems and is proven to be a very effective method when the experiment time and instability of volume are not concerns for the assay. The enrichment technique is especially well suited for biological applications that require cell culturing which inherently takes time so that the waiting time for droplet evaporation is not a concern. Such an exemplary application was shown by Ebrahimi and Alam in 2016 [26]. They showed that using the droplet impedance monitoring system, the osmotic response of bacterial cells to varying medium conditions can be measured as an alternative method to determine cell viability. The osmoregularity response of bacteria (*E. coli*, *S. epidermidis*, and *S. typhimurium*) were generated by evaporation of the droplet while monitoring the impedance change and deriving the electrical properties of the solution and cells. For dead cells, the cell membrane was compromised and solutes were free to transport across the membrane whereas in viable cultures active osmotic response of cells modulated the solution conductivity which was continuously monitored with the integrated electrodes.

5.2. Electrochemical Sensing

Electrical sensing of droplets was also shown using electrochemical sensing (Figure 5b). Electrochemical sensing is closely related to impedimetric change and can be confused with impedimetric studies. In this article, we discuss electrochemical sensing articles that utilize electroactive species [77]. There are three main types of electrochemical detection: amperometric, potentiometric and conductometric. As the name implies, the electrical property that is monitored is different for these techniques.

An early work on electrochemical sensing of microdroplets was carried out by Cai and Cooper et al. [78]. They showed a microchamber with two integrated electrodes (counter and reference electrodes were combined) for amperometric analysis of lactate. The sample solution was pipetted into the chamber that is covered by oil to prevent evaporation. Measurements were performed with droplets containing lactate, either spiked or generated as a metabolite by individual heart cells inside droplets. The study demonstrated that lactate can be detected at very low volumes by miniaturizing the electrodes and the working sample.

Label-free electrochemical detection of droplets was mostly used for segmented droplet systems. A major challenge in such systems is to have a nice contact between the liquid sample, i.e., the droplet, and the measurement electrodes. The early examples of such systems used electrodes that are pierced into the microchannel that probe the droplet that is aligned with the electrodes. Han and Zheng et al. [79] and Gu and Ding et al. [80] used such an approach to integrate amperometric sensing with PDMS microfluidic segmented droplet devices using platinum and gold electrodes, respectively. Han et al. used guidance microchannels to facilitate the insertion of the electrodes into the microchannel.

Sassa and Suzuki et al. showed a segmented flow system for coulometric detection inside droplets by squeezing the droplets into the sensing region for better contact [81]. Liquid droplets of discrete volumes were formed using syringe pumps and an auxiliary side channel inside microchannels. The droplets were transferred to the sensing region that has a shallower channel section to allow for

better positioning of the sample over the electrochemical sensing region. Different types of sensor geometries were fabricated and coulombic detection of hydrogen peroxide was shown for analysis of oxidase substrates. The working electrodes designed as an array of thin electrodes gave the best results in terms of sensitivity.

Lin and Chen et al. used a very novel approach to get around the contact problem [82]. They used standard glass/PDMS devices and a T-junction geometry to form segmented droplets. In the sensing section, they applied selective surface coatings so that the two-phase flow is converted into a laminar flow where the aqueous phase gets into contact with the bottom surface of the chip with the oil phase contacting the upper channel. The electrodes were placed underneath the channel and made a strong contact with the droplets. As an example of enzymatic kinetic study, they studied oxidation of glucose inside droplets by hydrogen peroxide (H_2O_2) measurement. By measuring the resultant H_2O_2 concentration for six different input glucose concentration levels, they were able to obtain the Lineweaver–Burke curve in 20 min.

Itoh and Suzuki et al. showed a very interesting application of amperometric detection using segmented flow droplets on a portable microfluidic device [83]. They have implemented a system for measurement of ATP concentration in fish (jack mackerel) extracts for quantification of freshness. They used a glass/PDMS device and formed aqueous droplets separated by air. By avoiding the use of an oil-based continuous solution, they avoided the contact problem between the sample and the electrodes. However, this sacrificed the control of sample integrity which heavily depends on the hydrophobicity of the channels. The droplets containing the sample and the substrate solutions were formed separately and merged before the detection region using the commonly used enlarging channel geometry. Detection was achieved using a three-electrode sensor with the enzymes (glycerol kinase and glycerol-3-phosphate oxidase) immobilized on the sensor itself which contains a Nafion membrane for additional selectivity. The system measures the amount of H_2O_2 concentration formed at the end of a two-step enzymatic reaction. The turn-around time of the system (from obtaining the sample to result) is around 30 min. Their results show that fish start losing ATP and hence, freshness, significantly after 5 h of death even if they are refrigerated.

The researchers have extended their study by further developing this system by measuring the K-value which is a metric used for quantitative assessment of ATP breakdown to uric acid through the concentration of byproducts of a series reactions [84]. They used two sensing sites to measure multiple reaction byproducts (Figure 6b). The freshness of jack mackerel, yellowtail, and sea bream was measured by comparing the results with HPLC measurements. Although it depends on the type of the fish, 5 h after death can be generalized as a threshold value for fresh fish.

Rattanarat and Chailapakul et al. have demonstrated that sensitivity of label-free droplet electrochemical sensing can be improved by modification of electrodes [85]. They used graphene/polyaniline nanocomposite to coat screen printed carbon paste electrodes to determine the amount of residual 4-aminophenol (4-AP) in commercial paracetamol formulations. The measurement potential voltage was optimized for chronoamperometric measurement. The system gave a very linear response to 4-AP concentration and was able to provide the required limit of detection determined by universal guidelines.

5.3. Resistive Pulse Sensing

Another label-free detection technique that was integrated to droplet fluidics is resistive pulse sensing (RPS). RPS is a technique forming the foundation of Coulter counting principle. It was very successfully combined with a segmented droplet fluidic platform by Gibb and Albrecht et al. as shown in Figure 5c [86]. They used two glass nanopores that were pulled from quartz capillaries and pierced to the PDMS microchannel from two side walls as shown in Figure 6c. One of the pores was used for material transport while the other was used for the electrical reference signal. The pore diameter was 24 nm. In addition to routine droplet size characterization, they showed that they can transfer DNA fragments of 10-kbp in and out of the droplet. The number of DNA fragments removed or

injected is a function of the dwell time (changes with droplet size and velocity), applied potential and DNA concentration. In addition to this article, there are also studies in the literature that show the characterization of microdroplets in emulsions using standard resistive pulse sensing units [87]. Since these systems do not use any of the droplet platforms explained in this review, we do not discuss them.

5.4. Microwave Sensing

Yesiloz, Boybay, and Ren have demonstrated a novel label-free sensing mechanism by combining a segmented flow system with microwave sensing as schematically shown in Figure 5d [88]. They used a microwave resonator that is composed of two concentric circular electrodes (Figure 6d). The outer electrode was excited and the change in resonance frequency was measured from the other electrode. They used a custom-made microwave circuitry to detect the frequency change which is a function of electrical properties of the medium inside the microchannel that is placed over the sensor. The system operates at high frequencies (at GHz range) and provides a high signal-to-noise ratio compared to MHz-range frequency impedimetric characterization systems. They have extensively characterized the performance of the system using droplets of varying glucose, potassium chloride solutions as well as with droplets using biological samples and antibacterial solutions. They have shown that the use of high-frequency signal provides high sensitivity even in high throughput droplet systems.
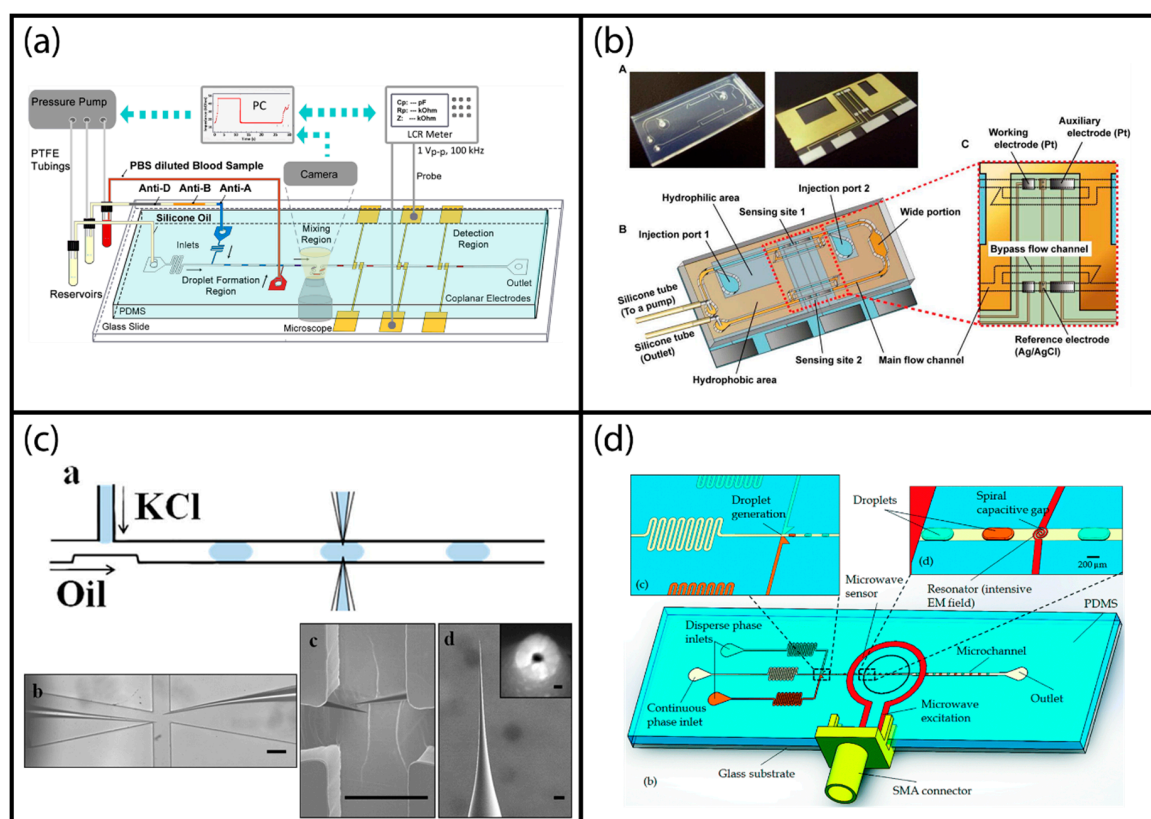

Figure 6. Examples of label-free electrical droplet detection: (**a**) Impedimetric detection of hemagglutination inside segmented droplets; reproduced from [73]. (**b**) Electrochemical detection of ATP concentration in fish extracts to determine fish freshness; reprinted with permission from [84]. American Chemical Society (2013). (**c**) Resistive pulse sensing integrated to a segmented droplet system using quartz capillaries; adapted with permission from [86]. Copyright 2014 American Chemical Society. (**d**) Microwave sensing of segmented droplets at GHz range; adapted from [88] with permission of The Royal Society of Chemistry.

6. Mass Spectrometry

Mass spectroscopy (MS) is a powerful technique for molecular analysis. It can provide detailed information regarding protein structure and function, enzyme reactions, biomarker identification, and contamination analysis for foods, beverages, soil etc. Such a wide range of test capability makes MS particularly interesting for droplet fluidic systems. A major downside of label-free MS analysis of droplets is the fact that it is a destructive measurement method. Therefore, it is an end-point detection rather than a flexible detection method that can be integrated into the droplet assay flow.

The only interface that is required between a droplet fluidic system and the mass spectroscopy devices is the ionization of the sample. Ionization at ambient conditions is an active field of research and is a developing field. In this review, we limit our discussion to more standardized ionization methods that can be integrated with multiple types of droplet platforms. Amongst various ionization methods, two techniques stand out: matrix-assisted laser desorption/ionization (MALDI) and electrospray ionization (ESI) as schematically shown in Figure 7a,b, respectively.
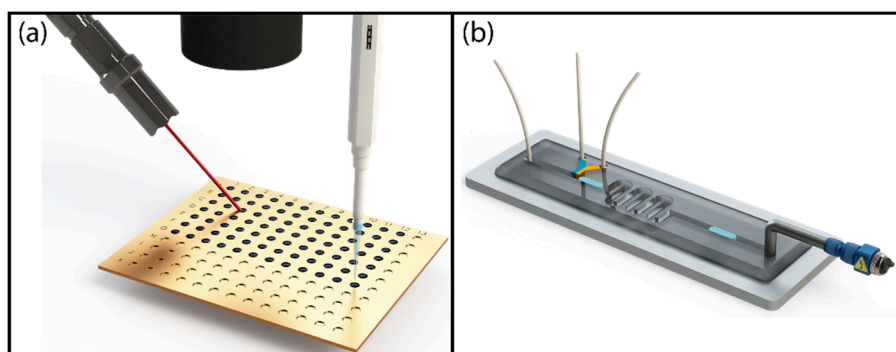

Figure 7. Schematic illustration of label-free mass spectroscopic detection techniques: (**a**) matrix-assisted laser desorption/ionization (MALDI) MS; (**b**) electrospray ionization (ESI) MS.

6.1. Matrix-Assisted Laser Desorption/Ionization (MALDI) MS

MALDI MS, which is usually preferred for analysis of larger molecules such as peptides, requires the sample to be mixed with a matrix which absorbs UV light (Figure 7a). The UV irradiation increases the temperature of the sample/matrix solution placed on a MALDI target as arrays of droplets. The rapid increase in temperature desorbs and ionizes the sample and allows analysis using the time-of-flight measurement principle. For most standard MS analyzers, the sample volume is around 1 µL. As described in Section 2.3, digital droplet systems move droplets on an array of electrodes. Since both MALDI-MS and digital microfluidic systems are array-based systems, their integration were the first examples of MS analysis of droplets.

The first example of droplet fluidics and MALDI-MS was from Wheeler and Garrell et al. in 2004 [89]. They used a parallel-plate configuration in which droplets of 0.5 µL are exposed to air, i.e., no oil immersion. They evaluated the ability of a digital droplet platform to move the matrix/sample solution to eliminate the manual sample processing and pipetting steps. Therefore, this is a study exploring the material compatibilities for both technologies. They investigated the potential MALDI matrices that are compatible with the digital droplet systems. They found out that droplets with up to 15% acetonitrile concentration have the sufficient contact angle change with electrical actuation which would allow them to be manipulated on a digital droplet system. The commonly used 2,5-dihydroxybenzoic acid (DHB) matrix was not compatible with droplet platforms. When they compared the MS analysis of standard MALDI targets and digital droplet/MALDI targets, they concluded that the latter had lower noise level, but slightly poorer resolution.

The same group has demonstrated the improvement of this platform for in-line sample purification for sensitive MALDI-MS analysis [90]. They used dispensing and digital droplet systems to generate

the droplets and purify them, respectively. Peptide solution droplets were formed on the digital droplet platform by manual pipetting. Then, the droplets were moved to a specific spot and dried. Later, a DI droplet was positioned over the same spot to dissolve and remove the hydrophilic impurities. Finally, another droplet of MALDI matrix was positioned on the same spot and dried. The dried spot was analyzed by MALDI-MS. They demonstrated that even with rinsing using a single DI droplet, dramatic improvement was achieved in MS results, which is critical for dilute protein sample analysis. Later on, they incorporated a droplet generation step for this platform to make it an all-electronic controlled system as a pure digital droplet system [91].

Nichols and Gardeniers demonstrated a similar digital droplet system which uses manually pipetted droplets to study fast enzymatic reactions using MALDI-MS [92]. The system combined two droplets to initiate a model protein enzymatic reaction and then another droplet is merged to quench the reaction. Finally, the droplet was made ready for MALDI-MS analysis by merging it with another droplet of MALDI matrix. They achieved mixing of droplet contents using electrohydrodynamic flow initiated by the integrated electrodes.

In order to overcome the potential cross-contamination effects of digital droplet platforms, MALDI-MS characterization was used by Yang and Wheeler et al. [93]. They demonstrated that repetitive droplet motion over the same electrodes may lead to contamination due to adsorption from the droplet to the surface and desorption from the surface to the droplet. They proposed a replaceable polymer skin to alleviate this problem and enabled the reusability of the electrode platform. After completing the droplet manipulation on the droplet platform, the skin was removed and placed onto a MALDI target plate followed by the MALDI-MS analysis.

The use of MALDI-MS for segmented flow systems was also demonstrated, although in principle, it is much easier to be applied for dispensed or digital droplet systems in which the droplets are already positioned on a planar surface instead of confining them in microchannels. Still, integration of segmented flow systems with MALDI-MS detection was successfully demonstrated through droplet deposition units. The first example of such a system was demonstrated by Rustem Ismagilov's group where droplets are formed, stored and injected into tubings rather than microchannels [94]. Finally, the droplets were deposited onto standard MALDI plates, evaporated and then a matrix solution was deposited onto the dried spots and dried a second time before analysis. It is important to note that this system used segmented droplet fluidics and dispensing droplet platforms to obtain the MALDI-MS targets.

More recently, a similar setup was demonstrated by Küster and Dittrich et al. that used high-density MALDI plates with 26444 circular hydrophilic spots of 300 μm diameter achieving oil phase separation passively on the MALDI plates [95]. The sample was dried in less than 60 s using nitrogen gas blow. The matrix was introduced to the analysis spot through the use of an automated X-Y stage positioner which was also used in the droplet deposition step (Figure 8a). The droplet dispensing module used an integrated optical droplet detection unit.

Pereira, Niu, and deMello reported a segmented flow droplet system to couple liquid chromatography (LC) to MALDI-MS analysis [24]. Compared to conventional interfaces, this novel droplet interface provided 50% improvement in the analytical performance of trypsin-digested proteins (Cytochrome C and BSA). De-emulsification of sample droplets was achieved by a hydrophobic and oleophilic membrane. First, the LC effluent was formed into microdroplets together with the MALDI matrix using a T-junction merging geometry. After mixing of the droplet content, the oil phase was removed by the membrane and the droplets were deposited on a MALDI plate using a micropositioning stage.

6.2. Electrospray Ionization (ESI) MS

Another common method for sample ionization for MS analysis is electrospray ionization (ESI), which uses high voltage for ionization (Figure 7b). Several studies have demonstrated on-line integration of segmented flow droplet systems to electrospray ionization mass spectroscopy units.

The main challenge in such a coupling is the extraction of the aqueous phase which may hinder Taylor cone formation due to the presence of surfactants or fluorocarbons. Therefore, for successful ionization of droplets using electrospraying, the non-sample medium (which is usually an oil-based continuous phase) should be isolated. Fidalgo and Huck et al. have achieved this by using a parallel sheet flow and by directing the droplet of interest to the aqueous phase using electrokinetic forces [96]. Droplets being pushed out of the oil phase merge with the aqueous phase. Then, droplets were fed to the ESI-MS analyzer through a fused-silica capillary emitter inserted into a steel sheath. This was a pioneering work from Wilhelm Huck's group.

In another work, Kelly and Smith et al. demonstrated the use of interfacial tension to transfer the dispersed aqueous phase droplets to a neighboring channel with continuous flow separated from the two-phase flow channel by linearly positioned microposts [97]. The system achieved passive droplet transfer to a side channel which was coupled to a downstream electrospray injection unit.

Zhu and Fang used a hydrophilic region covering approximately one-fourth of the main channel width, called the hydrophilic tongue, to direct the segmented samples to the electrospray ionization module [98]. They used an all-glass device and were able to selectively modify the surface properties so that the droplet content could be transferred to MS with minimal leakage of the oil phase. Through pressure control regulation, they were able to control the transfer ratio of the droplet to the ESI-MS unit: either complete or partial transfer. This system demonstrated droplet transfer rates up to 10 Hz and was utilized to monitor peptide alkylation reactions.

Robert Kennedy's group has demonstrated several examples of segmented droplet ESI-MS analysis systems. They used the standard T-junction droplet generator [99] as well as simplistic Teflon tubing integrated with a micropositioner and a syringe pump in the withdrawal mode [100,101] to form segmented samples inside the tubing which facilitated the coupling of the fluidic unit to the MS analyzer. They have reported sample segmentation with both air [100] and perfluorinated oil [99,101] as the continuous phase. Injection of other solutions into the droplets was achieved using Tee connectors [101]. They directly coupled this capillary to a commercial platinum coated fused silica nanospray emitter. The stability and monodispersity of the droplets were significantly improved when oil was used instead of air as the continuous phase. As an application, they screened acetylcholinesterase (AchE) inhibitors [100] and cathepsin B inhibitors [101].
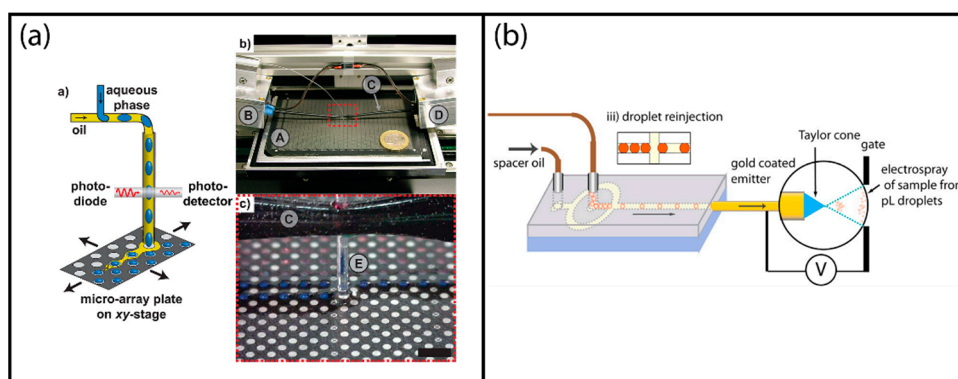

Figure 8. Examples of label-free mass spectroscopic droplet detection: (**a**) Matrix-assisted laser desorption/ionization (MALDI) MS analysis of segmented droplets transferred on a MALDI plate; reprinted with permission from [95]. American Chemical Society (2013). (**b**) Direct electrospray ionization (ESI) MS analysis of surfactant-stabilized segmented droplets; adapted with permission from [102]. American Chemical Society (2013).

More recently, direct injection of microdroplets without de-emulsification was also demonstrated in an effort to increase the throughput. Smith and Huck et al. used a commercial tri-block copolymer to suppress the noise from the oil phase and obtained analysis rates up to 10 Hz by directly coupling

the droplets through a reinjection module as schematically shown in Figure 8b [102]. They tested the system using antibody (Trastuzumab)-containing droplets of approximately 400 pL volume. The results obtained from the droplet system were compared to conventionally sprayed sample solutions and very similar results were obtained.

7. Other Label-free Droplet Sensing Methods

Apart from the above-mentioned commonly used tools, there are other label-free droplet sensing systems. In this section, a selection of these systems is given. We would like to emphasize that our classification is solely based on the commonality of the approach such that the studies listed in this section are less frequently used techniques compared to the methods explained in the previous sections.

7.1. Nuclear Magnetic Resonance (NMR) Spectroscopy

Droplet fluidic systems have also been integrated with nuclear magnetic resonance (NMR) spectroscopy. Similar to MS, NMR is a very advanced characterization system which is standard across chemical analysis laboratories. However, there is a major difference between NMR and MS for droplet analysis. Unlike MS analysis, flow through NMR devices allow the sample to be recollected for further analysis. Thus, NMR characterization can be integrated within a sequential droplet analysis workflow.

Kautz, Goetzinger, and Karger explain a system for the analysis of segmented flow droplets using a microcoil probe which is more sensitive due to reduced coil diameter and reduced noise [103]. The droplet samples were formed inside tubings using a fluid handling unit. Sample solutions were placed in a 96-well plate. The droplets were transferred to the NMR probe and the flow was stopped when droplets were centered on the NMR coil. In this study, they tested the throughput of the unit for sequential analysis of samples. They also checked cross-contamination between droplets. This study concluded that high throughput NMR analysis of segmented droplets can be achieved at a rate of 1.5 min/sample including the sample change time. Compared to the commercial high throughput NMR methods, segmented flow integrated NMR yields 20-fold less solvent consumption. As pointed out by this article, the main benefit of segmented flow droplet NMR analysis is preventing the sample dispersion or sample loss experienced in other continuous flow type NMR systems.

Lin and Kautz et al. have further improved this system for trace chemical detection [104]. In this study, the authors present a high-end analysis tool which can perform MS analysis and segmented flow NMR followed by LC. 98% of the sample was used for droplet microcoil measurement, whereas 2% was needed for ESI-MS. The authors showed analysis of a bioactive cyanobacterial extract in addition to the reproducibility and performance characterization results obtained by known quantities of drugs: cycloheximide, indapamide, digitoxin, and taxol. As in the previous work, a fluorocarbon oil continuous phase was used, and wash plugs were formed to prevent cross-contamination between sample plugs. A commercially available NMR probe was used in this study.

In 2013, Kautz, Wang, and Giese demonstrated NMR analysis of very low volume samples for DNA adduct characterization [105]. Only 1.5 µL of sample was used for the analysis. Although most commercial microcoil probes use sample volumes on the order of microliters, there is still significant dead volume due to sample loading and adhesion to the tubing walls. The use of segmented droplets eliminates all these problems. They have shown the acquisition of 1D and 2D spectra as a complementary technique to MS for identification of adduct structure.

7.2. X-ray Diffraction/Scattering Analysis

X-ray diffraction and scattering analysis give the atomic structure of crystalline materials. The integration of droplet systems with X-ray analysis devices bares challenges similar to NMR that is mostly about interfacing. Rustem Ismagilov's group has shown fascinating examples of such integration that resulted in a commercial system called CrystalCards® droplet chips by Protein BioSolutions.

They showed the very first crystallographic characterization of protein crystals formed inside a segmented droplet system in 2004 [106]. They used a T-junction geometry, where they were able to

change the ratio of the protein solution and the precipitant to find the optimal concentration of the mix. They achieved protein crystallization by vapor diffusion inside capillaries using alternating droplets of the sample and high concentration salt solutions. Using thin-walled capillaries, they were able to get in-line XRD measurements to screen crystal formation conditions by avoiding the manual handling of the formed crystals [107].

Stehle and Seiffert et al. showed a similar study where detection of segmented droplets was performed by a small angle X-ray scattering (SAXS) system [108]. SAXS is used to probe the size, structure, and concentration of particles. In this example, gold nanoparticles in aqueous solutions were characterized using two segmented flow systems. In the first one, PDMS chips were used and pre-formed nanoparticles were loaded into droplets as the dispersed phase and then the outlet of the chip is coupled to SAXS detectors. Rectangular and circular detection tubes with a wall thickness of just 10 mm were used. For the second system, glass capillaries were used to form segmented droplets and nanoparticle synthesis was also achieved inside droplets. Then, droplets were directed to the SAXS detection unit. This study highlights an important distinction between PDMS segmented flow systems and glass capillary-type systems. When glass capillaries were used to generate the droplets, the choice of materials was less restricted in comparison to porous PDMS devices which swell with solvents. The outputs of both systems were coupled to the SAXS detection and the spectra were obtained successfully. An elliptical shape X-ray beam was used to reduce artifacts due to the capillary walls. Model experiments for both systems were provided in this study to prove the ability to use SAXS for segmented droplet experiments.

As seen from the examples given in this section, when droplets are required to be characterized by conventional instruments, the major issue is interfacing the droplets with the measurement platform. For such examples, the droplets formed inside tubings, i.e., segmented droplet systems, are advantageous since droplets can be transferred between tubings that may have different diameters and are made up of different materials. Hence, the interfacing of droplet samples can be handled relatively easily. Additionally, since most of the instruments have a long distance between sample introduction port and the measurement section, droplets should confine the integrity of the sample plug by avoiding sample dispersion [109]. Therefore, segmented flow droplets seem to be the best choice for integration of droplet platforms with advanced characterization systems.

8. Discussion and Conclusions

Droplet microfluidic platforms and their applications show a wide variety. Most studies in this field were published by multi-disciplinary teams that can bring together multiple modalities for a given application. The main concern when designing a droplet system is determining the droplet platform and the detection scheme to be used. As seen in this review, this decision is strongly coupled, and specifications of the whole system should be taken into account. For most biochemical analysis systems, the first consideration when determining the type of detection system is the limit of detection, sensitivity, specificity and dynamic range for the analyte that is being detected. These metrics heavily rely on the type of the instrument that is used and its coupling with the droplet fluidic system; therefore, it is not easy to draw an absolute comparison between different methods. Cost, portability and the need for calibration are some other concerns that should be evaluated considering the specifications of a given application. We hope the literature provided in this article would be a good starting point for researchers designing a system from scratch.

Another major criterion when selecting the detection system is the throughput that is required, i.e., the number of droplets to be sensed in a given time. Droplet fluidic platforms can generate a vast amount of data from small amounts of liquid by high droplet generation rate abilities. The advancing droplet technology platforms put a burden on the detection systems to analyze each and every droplet at high speeds, preferably at rates matching the droplet generation rate so that real-time analysis is possible. Therefore, continuous improvement is needed in the label-free detection techniques to keep up with the advancements in droplet technologies, so that the detection module is not the limiting part

of an integrated system. For very high throughput applications, array-based detection systems, such as image-processing-based optical detection, are favorable. However, most detection platforms have singular detection units and multiplexing is achieved by placing multiple sensors on the same device. For such a case, the footprint of the sensor is an important concern together with the potential cross-talk between closely placed sensors. In that respect, electrical sensing platforms, especially impedimetric detection, are quite advantageous due to the know-how accumulated in microfabrication of electronic circuitries and sensors.

One of the concerns that should be taken into account when selecting a label-free detection method is the degree of design change required in the fluidic architecture. The ability to decouple the fluidic design from the sensor design allows the system to be more flexible so that the fluidics, which can be challenging for some droplet systems, especially when complex samples are being used, and the sensor design can be modified independently. If the two systems are coupled, design changes would be more time- and budget-consuming. Non-contact detection techniques are more favorable in this regard. Also, the compatibility of the detection scheme to the droplet platform should be evaluated which would facilitate the integration of fluidics with the sensor. For instance, implementation of impedimetric detection on digital droplet systems was one of the first examples of label-free detection examples, since the basic digital droplet system already houses the electronics required for droplet motion.

So far, the main goal of the droplet sensor platforms was to achieve high sensitivity for certain biochemical applications of droplet fluidic systems. Recently, exciting developments have been reported in analysis of nucleic acids (DNA, RNA, miRNA) as well as nanoscale vesicles such as exosomes. Therefore, there is a need for further shrinking down of the size of the droplets so that these extremely low concentration analytes can yield detectable signals inside much smaller confined volumes. Most of the studies reported in the literature use droplets with dimensions of tens to hundred-micron scales. We believe the next challenge for the scientific community would be to develop methods for droplet manipulation and sensing at the nanoscale. In addition, integration of organic photodiodes [110,111] and nanowire- [112] or graphene- [113,114] based field effect transistors with droplet fluidic platforms may open new avenues. Although we have seen some integration of these novel optical and electrical sensing modalities in microfluidics, their adaptation by droplet-based platforms have remained limited, thus demonstrating a potential for future label-free droplet sensing studies.

Author Contributions: C.E. and A.K. designed the outline of the manuscript. A.K. and A.S. performed the literature search. C.E. wrote the majority of the manuscript. A.S. prepared the figures. Discussions on mass spectroscopy and vibrational spectroscopy were written by A.S. and A.K. All authors reviewed and edited the manuscript.

Conflicts of Interest: The authors declare no conflict of interest.

References

1. Whitesides, G.M. The origins and the future of microfluidics. *Nature* **2006**, *442*, 368–373. [CrossRef] [PubMed]
2. Squires, T.M.; Quake, S.R. Microfluidics: Fluid physics at the nanoliter scale. *Rev. Mod. Phys.* **2005**, *77*, 977–1026. [CrossRef]
3. Theberge, A.B.; Courtois, F.; Schaerli, Y.; Fischlechner, M.; Abell, C.; Hollfelder, F.; Huck, W.T.S. Microdroplets in microfluidics: An evolving platform for discoveries in chemistry and biology. *Angew. Chem. Int. Ed.* **2010**, *49*, 5846–5868. [CrossRef] [PubMed]
4. Teh, S.Y.; Lin, R.; Hung, L.H.; Lee, A.P. Droplet microfluidics. *Lab Chip* **2008**, *8*, 198–220. [CrossRef] [PubMed]
5. Dressler, O.J.; Maceiczyk, R.M.; Chang, S.I.; deMello, A.J. Droplet-based microfluidics: Enabling impact on drug discovery. *J. Biomol. Screen.* **2014**, *19*, 483–496. [CrossRef] [PubMed]

6. Cao, L.; Cui, X.Y.; Hu, J.; Li, Z.D.; Choi, J.R.; Yang, Q.Z.; Lin, M.; Ying, H.L.; Xu, F. Advances in digital polymerase chain reaction (DPCR) and its emerging biomedical applications. *Biosens. Bioelectron.* **2017**, *90*, 459–474. [CrossRef] [PubMed]

7. Dong, L.H.; Meng, Y.; Sui, Z.W.; Wang, J.; Wu, L.Q.; Fu, B.Q. Comparison of four digital PCR platforms for accurate quantification of DNA copy number of a certified plasmid DNA reference material. *Sci. Rep.* **2015**, *5*, 13174. [CrossRef] [PubMed]

8. Shang, L.; Cheng, Y.; Zhao, Y. Emerging droplet microfluidics. *Chem. Rev.* **2017**, *117*, 7964–8040. [CrossRef] [PubMed]

9. Christopher, G.F.; Anna, S.L. Microfluidic methods for generating continuous droplet streams. *J. Phys. D Appl. Phys.* **2007**, *40*, R319. [CrossRef]

10. Vladisavljević, G.; Kobayashi, I.; Nakajima, M. Production of uniform droplets using membrane, microchannel and microfluidic emulsification devices. *Microfluid. Nanofluid.* **2012**, *13*, 151–178. [CrossRef]

11. Zhu, P.; Wang, L. Passive and active droplet generation with microfluidics: A review. *Lab Chip* **2017**, *17*, 34–75. [CrossRef] [PubMed]

12. Pit, A.M.; Duits, M.H.; Mugele, F. Droplet manipulations in two phase flow microfluidics. *Micromachines* **2015**, *6*, 1768–1793. [CrossRef]

13. Xi, H.-D.; Zheng, H.; Guo, W.; Gañán-Calvo, A.M.; Ai, Y.; Tsao, C.-W.; Zhou, J.; Li, W.; Huang, Y.; Nguyen, N.-T. Active droplet sorting in microfluidics: A review. *Lab Chip* **2017**, *17*, 751–771. [CrossRef] [PubMed]

14. Isiksacan, Z.; Guler, M.T.; Kalantarifard, A.; Asghari, M.; Elbuken, C. Lab-on-a-Chip Platforms for Disease Detection and Diagnosis. In *Biosensors and Nanotechnology: Applications in Health Care Diagnostics*; Altintas, Z., Ed.; John Wiley & Sons: Hoboken, NJ, USA, 2017; pp. 155–181. [CrossRef]

15. Joensson, H.N.; Andersson Svahn, H. Droplet microfluidics—A tool for single-cell analysis. *Angew. Chem. Int. Ed.* **2012**, *51*, 12176–12192. [CrossRef] [PubMed]

16. Lagus, T.P.; Edd, J.F. A review of the theory, methods and recent applications of high-throughput single-cell droplet microfluidics. *J. Phys. D Appl. Phys.* **2013**, *46*, 114005. [CrossRef]

17. Dressler, O.; Casadevall i Solvas, X.; deMello, A.J. Chemical and biological dynamics using droplet-based microfluidics. *Ann. Rev. Anal. Chem.* **2017**, *10*, 1–24. [CrossRef] [PubMed]

18. Gach, P.C.; Iwai, K.; Kim, P.W.; Hillson, N.J.; Singh, A.K. Droplet microfluidics for synthetic biology. *Lab Chip* **2017**, *17*, 3388–3400. [CrossRef] [PubMed]

19. Garcia-Cordero, J.L.; Fan, Z.H. Sessile droplets for chemical and biological assays. *Lab Chip* **2017**, *17*, 2150–2166. [CrossRef] [PubMed]

20. Wildgen, S.M.; Dunn, R.C. Whispering gallery mode resonators for rapid label-free biosensing in small volume droplets. *Biosensors* **2015**, *5*, 118–130. [CrossRef] [PubMed]

21. Yin, L.; Wang, S.; Shan, X.; Zhang, S.; Tao, N. Quantification of protein interaction kinetics in a micro droplet. *Rev. Sci. Instrum.* **2015**, *86*, 114101. [CrossRef] [PubMed]

22. Ebrahimi, A.; Dak, P.; Salm, E.; Dash, S.; Garimella, S.V.; Bashir, R.; Alam, M.A. Nanotextured superhydrophobic electrodes enable detection of attomolar-scale DNA concentration within a droplet by non-faradaic impedance spectroscopy. *Lab Chip* **2013**, *13*, 4248–4256. [CrossRef] [PubMed]

23. Valentino, J.; Troian, S.; Wagner, S. Microfluidic Detection and Analysis by Integration of Evanescent Wave Sensing with Thermocapillary Actuation. In Proceedings of the 18th IEEE International Conference on Micro Electro Mechanical Systems (MEMS), Miami Beach, FL, USA, 30 January–3 February 2005; pp. 730–733.

24. Pereira, F.; Niu, X. A nano lc-maldi mass spectrometry droplet interface for the analysis of complex protein samples. *PLoS ONE* **2013**, *8*, e63087. [CrossRef] [PubMed]

25. Jarocka, U.; Radecka, H.; Malinowski, T.; Michalczuk, L.; Radecki, J. Detection of prunus necrotic ringspot virus in plant extracts with impedimetric immunosensor based on glassy carbon electrode. *Electroanalysis* **2013**, *25*, 433–438. [CrossRef]

26. Ebrahimi, A.; Alam, M.A. Evaporation-induced stimulation of bacterial osmoregulation for electrical assessment of cell viability. *Proc. Natl. Acad. Sci. USA* **2016**, *113*, 7059–7064. [CrossRef] [PubMed]

27. Zhu, Y.; Fang, Q. Analytical detection techniques for droplet microfluidics—A review. *Anal. Chim. Acta* **2013**, *787*, 24–35. [CrossRef] [PubMed]

28. Du, W.; Li, L.; Nichols, K.P.; Ismagilov, R.F. Slipchip. *Lab Chip* **2009**, *9*, 2286–2292. [CrossRef] [PubMed]

29. Malic, L.; Brassard, D.; Veres, T.; Tabrizian, M. Integration and detection of biochemical assays in digital microfluidic loc devices. *Lab Chip* **2010**, *10*, 418–431. [CrossRef] [PubMed]

30. Kaminski, T.S.; Garstecki, P. Controlled droplet microfluidic systems for multistep chemical and biological assays. *Chem. Soc. Rev.* **2017**, *46*, 6210–6226. [CrossRef] [PubMed]

31. Cole, R.H.; Tang, S.Y.; Siltanen, C.A.; Shahi, P.; Zhang, J.Q.; Poust, S.; Gartner, Z.J.; Abate, A.R. Printed droplet microfluidics for on demand dispensing of picoliter droplets and cells. *Proc. Natl. Acad. Sci. USA* **2017**, *114*, 8728–8733. [CrossRef] [PubMed]

32. Luka, G.; Ahmadi, A.; Najjaran, H.; Alocilja, E.; DeRosa, M.; Wolthers, K.; Malki, A.; Aziz, H.; Althani, A.; Hoorfar, M. Microfluidics integrated biosensors: A leading technology towards lab-on-a-chip and sensing applications. *Sensors* **2015**, *15*, 30011–30031. [CrossRef] [PubMed]

33. Neil, S.R.; Rushworth, C.M.; Vallance, C.; Mackenzie, S.R. Broadband cavity-enhanced absorption spectroscopy for real time, in situ spectral analysis of microfluidic droplets. *Lab Chip* **2011**, *11*, 3953–3955. [CrossRef] [PubMed]

34. Mao, Z.; Guo, F.; Xie, Y.; Zhao, Y.; Lapsley, M.I.; Wang, L.; Mai, J.D.; Costanzo, F.; Huang, T.J. Label-free measurements of reaction kinetics using a droplet-based optofluidic device. *J. Lab. Autom.* **2015**, *20*, 17–24. [CrossRef] [PubMed]

35. Hung, L.-H.; Choi, K.M.; Tseng, W.-Y.; Tan, Y.-C.; Shea, K.J.; Lee, A.P. Alternating droplet generation and controlled dynamic droplet fusion in microfluidic device for CDS nanoparticle synthesis. *Lab Chip* **2006**, *6*, 174–178. [CrossRef] [PubMed]

36. Srinivasan, V.; Pamula, V.K.; Fair, R.B. Droplet-based microfluidic lab-on-a-chip for glucose detection. *Anal. Chim. Acta* **2004**, *507*, 145–150. [CrossRef]

37. Srinivasan, V.; Pamula, V.K.; Fair, R.B. An integrated digital microfluidic lab-on-a-chip for clinical diagnostics on human physiological fluids. *Lab Chip* **2004**, *4*, 310–315. [CrossRef] [PubMed]

38. Hassan, S.-U.; Nightingale, A.M.; Niu, X. Continuous measurement of enzymatic kinetics in droplet flow for point-of-care monitoring. *Analyst* **2016**, *141*, 3266–3273. [CrossRef] [PubMed]

39. Bunaciu, A.A.; Aboul-Enein, H.Y.; Fleschin, Ş. Vibrational spectroscopy in clinical analysis. *Appl. Spectrosc. Rev.* **2015**, *50*, 176–191. [CrossRef]

40. Chan, K.A.; Niu, X.; DeMello, A.; Kazarian, S. Generation of chemical movies: Ft-ir spectroscopic imaging of segmented flows. *Anal. Chem.* **2011**, *83*, 3606–3609. [CrossRef] [PubMed]

41. Müller, T.; Ruggeri, F.S.; Kulik, A.J.; Shimanovich, U.; Mason, T.O.; Knowles, T.P.; Dietler, G. Nanoscale spatially resolved infrared spectra from single microdroplets. *Lab Chip* **2014**, *14*, 1315–1319. [CrossRef] [PubMed]

42. Barnes, S.E.; Cygan, Z.T.; Yates, J.K.; Beers, K.L.; Amis, E.J. Raman spectroscopic monitoring of droplet polymerization in a microfluidic device. *Analyst* **2006**, *131*, 1027–1033. [CrossRef] [PubMed]

43. Cristobal, G.; Arbouet, L.; Sarrazin, F.; Talaga, D.; Bruneel, J.-L.; Joanicot, M.; Servant, L. On-line laser raman spectroscopic probing of droplets engineered in microfluidic devices. *Lab Chip* **2006**, *6*, 1140–1146. [CrossRef] [PubMed]

44. Sarrazin, F.; Salmon, J.-B.; Talaga, D.; Servant, L. Chemical reaction imaging within microfluidic devices using confocal raman spectroscopy: The case of water and deuterium oxide as a model system. *Anal. Chem.* **2008**, *80*, 1689–1695. [CrossRef] [PubMed]

45. Bringer, M.R.; Gerdts, C.J.; Song, H.; Tice, J.D.; Ismagilov, R.F. Microfluidic systems for chemical kinetics that rely on chaotic mixing in droplets. *Philos. Trans. R. Soc. A* **2004**, *362*, 1087–1104. [CrossRef] [PubMed]

46. Jahn, I.J.; Zukovskaja, O.; Zheng, X.S.; Weber, K.; Bocklitz, T.W.; Cialla-May, D.; Popp, J. Surface-enhanced raman spectroscopy and microfluidic platforms: Challenges, solutions and potential applications. *Analyst* **2017**, *142*, 1022–1047. [CrossRef] [PubMed]

47. Marz, A.; Henkel, T.; Cialla, D.; Schmitt, M.; Popp, J. Droplet formation via flow-through microdevices in raman and surface enhanced raman spectroscopy-concepts and applications. *Lab Chip* **2011**, *11*, 3584–3592. [CrossRef] [PubMed]

48. Strehle, K.R.; Cialla, D.; Rösch, P.; Henkel, T.; Köhler, M.; Popp, J. A reproducible surface-enhanced raman spectroscopy approach. Online sers measurements in a segmented microfluidic system. *Anal. Chem.* **2007**, *79*, 1542–1547. [CrossRef] [PubMed]

49. Ackermann, K.R.; Henkel, T.; Popp, J. Quantitative online detection of low-concentrated drugs via a sers microfluidic system. *Chem. Phys. Chem.* **2007**, *8*, 2665–2670. [CrossRef] [PubMed]

50. Walter, A.; März, A.; Schumacher, W.; Rösch, P.; Popp, J. Towards a fast, high specific and reliable discrimination of bacteria on strain level by means of SERS in a microfluidic device. *Lab Chip* **2011**, *11*, 1013–1021. [CrossRef] [PubMed]

51. Wang, G.; Lim, C.; Chen, L.; Chon, H.; Choo, J.; Hong, J. Surface-enhanced raman scattering in nanoliter droplets: Towards high-sensitivity detection of mercury (ii) ions. *Anal. Bioanal. Chem.* **2009**, *394*, 1827–1832. [CrossRef] [PubMed]

52. Gao, R.; Choi, N.; Chang, S.-I.; Kang, S.H.; Song, J.M.; Cho, S.I.; Lim, D.W.; Choo, J. Highly sensitive trace analysis of paraquat using a surface-enhanced raman scattering microdroplet sensor. *Anal. Chim. Acta* **2010**, *681*, 87–91. [CrossRef] [PubMed]

53. Cecchini, M.P.; Hong, J.; Lim, C.; Choo, J.; Albrecht, T.; Demello, A.J.; Edel, J.B. Ultrafast surface enhanced resonance raman scattering detection in droplet-based microfluidic systems. *Anal. Chem.* **2011**, *83*, 3076–3081. [CrossRef] [PubMed]

54. Syme, C.D.; Martino, C.; Yusvana, R.; Sirimuthu, N.M.; Cooper, J.M. Quantitative characterization of individual microdroplets using surface-enhanced resonance raman scattering spectroscopy. *Anal. Chem.* **2012**, *84*, 1491–1495. [CrossRef] [PubMed]

55. Malic, L.; Veres, T.; Tabrizian, M. Two-dimensional droplet-based surface plasmon resonance imaging using electrowetting-on-dielectric microfluidics. *Lab Chip* **2009**, *9*, 473–475. [CrossRef] [PubMed]

56. Malic, L.; Veres, T.; Tabrizian, M. Biochip functionalization using electrowetting-on-dielectric digital microfluidics for surface plasmon resonance imaging detection of DNA hybridization. *Biosens. Bioelectron.* **2009**, *24*, 2218–2224. [CrossRef] [PubMed]

57. Arce, C.L.; Witters, D.; Puers, R.; Lammertyn, J.; Bienstman, P. Silicon photonic sensors incorporated in a digital microfluidic system. *Anal. Bioanal. Chem.* **2012**, *404*, 2887–2894. [CrossRef] [PubMed]

58. Wang, Y.B.; Su, L.Y.; Fu, C.S.; Huang, C.S.; Hsu, W. Droplet-based label-free detection system based on guided-mode resonance and electrowetting-on-dielectric for concentration measurement. *Jpn. J. Appl. Phys.* **2017**, *56*. [CrossRef]

59. Yin, L.L.; Wang, S.P.; Shan, X.N.; Zhang, S.T.; Tao, N.J. Quantification of protein interaction kinetics in a micro droplet. *Rev. Sci. Instrum.* **2015**, *86*, 114101. [CrossRef] [PubMed]

60. Glawdel, T.; Elbuken, C.; Ren, C.L. Droplet formation in microfluidic t-junction generators operating in the transitional regime. I. Experimental observations. *Phys. Rev. E* **2012**, *85*, 016322. [CrossRef] [PubMed]

61. Glawdel, T.; Elbuken, C.; Ren, C.L. Droplet formation in microfluidic t-junction generators operating in the transitional regime. II. Modeling. *Phys. Rev. E* **2012**, *85*, 016323. [CrossRef] [PubMed]

62. Basu, A.S. Droplet morphometry and velocimetry (DMV): A video processing software for time-resolved, label-free tracking of droplet parameters. *Lab Chip* **2013**, *13*, 1892–1901. [CrossRef] [PubMed]

63. Zang, E.; Brandes, S.; Tovar, M.; Martin, K.; Mech, F.; Horbert, P.; Henkel, T.; Figge, M.T.; Roth, M. Real-time image processing for label-free enrichment of actinobacteria cultivated in picolitre droplets. *Lab Chip* **2013**, *13*, 3707–3713. [CrossRef] [PubMed]

64. Hofmann, T.W.; Hänselmann, S.; Janiesch, J.-W.; Rademacher, A.; Böhm, C.H. Applying microdroplets as sensors for label-free detection of chemical reactions. *Lab Chip* **2012**, *12*, 916–922. [CrossRef] [PubMed]

65. Liao, T.-C.; Yeh, J.A. Microdroplet protein sensors on a gold surface with a self-assembled monolayer treatment. *Int. J. Autom. Smart Technol.* **2012**, *2*, 43–48. [CrossRef]

66. Chen, J.Z.; Darhuber, A.A.; Troian, S.M.; Wagner, S. Capacitive sensing of droplets for microfluidic devices based on thermocapillary actuation. *Lab Chip* **2004**, *4*, 473–480. [CrossRef] [PubMed]

67. Srivastava, N.; Burns, M.A. Electronic drop sensing in microfluidic devices: Automated operation of a nanoliter viscometer. *Lab Chip* **2006**, *6*, 744–751. [CrossRef] [PubMed]

68. Elbuken, C.; Glawdel, T.; Chan, D.; Ren, C.L. Detection of microdroplet size and speed using capacitive sensors. *Sens. Actuators A Phys.* **2011**, *171*, 55–62. [CrossRef]

69. Isgor, P.K.; Marcali, M.; Keser, M.; Elbuken, C. Microfluidic droplet content detection using integrated capacitive sensors. *Sens. Actuators B Chem.* **2015**, *210*, 669–675. [CrossRef]

70. Kemna, E.W.; Segerink, L.I.; Wolbers, F.; Vermes, I.; van den Berg, A. Label-free, high-throughput, electrical detection of cells in droplets. *Analyst* **2013**, *138*, 4585–4592. [CrossRef] [PubMed]

71. Simon, M.G.; Lin, R.; Lopez-Prieto, J.; Lee, A.P. Label-Free Detection of DNA Amplification in Droplets Using Electrical Impedance. In Proceedings of the 15th International Conference on Miniaturized Systems for Chemistry and Life Sciences, Seattle, WA, USA, 2–6 October 2011.

72. Lee, A.P.; Lopez-Prieto, J.; Lin, R.; Simon, M.; Martin, N. Real-Time, Label-Free Detection of Nucleic Acid Amplification in Droplets Using Impedance Spectroscopy and Solid-Phase Substrate. U.S. Patent US9030215B2, 12 May 2015.

73. Marcali, M.; Elbuken, C. Impedimetric detection and lumped element modelling of a hemagglutination assay in microdroplets. *Lab Chip* **2016**, *16*, 2494–2503. [CrossRef] [PubMed]

74. Sadeghi, S.; Ding, H.J.; Shah, G.J.; Chen, S.P.; Keng, P.Y.; Kim, C.J.; van Dam, R.M. On chip droplet characterization: A practical, high-sensitivity measurement of droplet impedance in digital microfluidics. *Anal. Chem.* **2012**, *84*, 1915–1923. [CrossRef] [PubMed]

75. Shih, S.C.C.; Barbulovic-Nad, I.; Yang, X.N.; Fobel, R.; Wheeler, A.R. Digital microfluidics with impedance sensing for integrated cell culture and analysis. *Biosens. Bioelectron.* **2013**, *42*, 314–320. [CrossRef] [PubMed]

76. Ernst, A.; Streule, W.; Schmitt, N.; Zengerle, R.; Koltay, P. A capacitive sensor for non-contact nanoliter droplet detection. *Sens. Actuators A Phys.* **2009**, *153*, 57–63. [CrossRef]

77. Luo, C.X.; Yang, X.J.; Fu, O.; Sun, M.H.; Ouyang, Q.; Chen, Y.; Ji, H. Picoliter-volume aqueous droplets in oil: Electrochemical detection and east electroporation. *Electrophoresis* **2006**, *27*, 1977–1983. [CrossRef] [PubMed]

78. Cai, X.X.; Klauke, N.; Glidle, A.; Cobbold, P.; Smith, G.L.; Cooper, J.M. Ultra-low-volume, real-time measurements of lactate from the single heart cell using microsystems technology. *Anal. Chem.* **2002**, *74*, 908–914. [CrossRef] [PubMed]

79. Han, Z.Y.; Li, W.T.; Huang, Y.Y.; Zheng, B. Measuring rapid enzymatic kinetics by electrochemical method in droplet-based microfluidic devices with pneumatic valves. *Anal. Chem.* **2009**, *81*, 5840–5845. [CrossRef] [PubMed]

80. Gu, S.; Lu, Y.; Ding, Y.; Li, L.; Zhang, F.; Wu, Q. Droplet-based microfluidics for dose–response assay of enzyme inhibitors by electrochemical method. *Anal. Chim. Acta* **2013**, *796*, 68–74. [CrossRef] [PubMed]

81. Sassa, F.; Laghzali, H.; Fukuda, J.; Suzuki, H. Coulometric detection of components in liquid plugs by microfabricated flow channel and electrode structures. *Anal. Chem.* **2010**, *82*, 8725–8732. [CrossRef] [PubMed]

82. Lin, X.Y.; Hu, X.Q.; Bai, Z.Q.; He, Q.H.; Chen, H.W.; Yan, Y.Z.; Ding, Z.H. A microfluidic chip capable of switching w/o droplets to vertical laminar flow for electrochemical detection of droplet contents. *Anal. Chim. Acta* **2014**, *828*, 70–79. [CrossRef] [PubMed]

83. Itoh, D.; Sassa, F.; Nishi, T.; Kani, Y.; Murata, M.; Suzuki, H. Droplet-based microfluidic sensing system for rapid fish freshness determination. *Sens. Actuators B Chem.* **2012**, *171*, 619–626. [CrossRef]

84. Itoh, D.; Koyachi, E.; Yokokawa, M.; Murata, Y.; Murata, M.; Suzuki, H. Microdevice for on-site fish freshness checking based on k-value measurement. *Anal. Chem.* **2013**, *85*, 10962–10968. [CrossRef] [PubMed]

85. Rattanarat, P.; Suea-Ngam, A.; Ruecha, N.; Siangproh, W.; Henry, C.S.; Monpichar, S.A.; Chailapakul, O. Graphene-polyaniline modified electrochemical droplet-based microfluidic sensor for high-throughput determination of 4-aminophenol. *Anal. Chim. Acta* **2016**, *925*, 51–60. [CrossRef] [PubMed]

86. Gibb, T.R.; Ivanov, A.P.; Edel, J.B.; Albrecht, T. Single molecule ionic current sensing in segmented flow microfluidics. *Anal. Chem.* **2014**, *86*, 1864–1871. [CrossRef] [PubMed]

87. Somerville, J.A.; Willmott, G.R.; Eldridge, J.; Griffiths, M.; McGrath, K.M. Size and charge characterisation of a submicrometre oil-in-water emulsion using resistive pulse sensing with tunable pores. *J. Colloid Interface Sci.* **2013**, *394*, 243–251. [CrossRef] [PubMed]

88. Yesiloz, G.; Boybay, M.S.; Ren, C.L. Label-free high-throughput detection and content sensing of individual droplets in microfluidic systems. *Lab Chip* **2015**, *15*, 4008–4019. [CrossRef] [PubMed]

89. Wheeler, A.R.; Moon, H.; Kim, C.J.; Loo, J.A.; Garrell, R.L. Electrowetting-based microfluidics for analysis of peptides and proteins by matrix-assisted laser desorption/ionization mass spectrometry. *Anal. Chem.* **2004**, *76*, 4833–4838. [CrossRef] [PubMed]

90. Wheeler, A.R.; Moon, H.; Bird, C.A.; Loo, R.R.O.; Kim, C.J.; Loo, J.A.; Garrell, R.L. Digital microfluidics with in-line sample purification for proteomics analyses with MALDI-MS. *Anal. Chem.* **2005**, *77*, 534–540. [CrossRef] [PubMed]

91. Moon, H.; Wheeler, A.R.; Garrell, R.L.; Loo, J.A.; Kim, C.J. An integrated digital microfluidic chip for multiplexed proteomic sample preparation and analysis by MALDI-MS. *Lab Chip* **2006**, *6*, 1213–1219. [CrossRef] [PubMed]

92. Nichols, K.P.; Gardeniers, H.J.G.E. A digital microfluidic system for the investigation of pre-steady-state enzyme kinetics using rapid quenching with MALDI-TOF mass spectrometry. *Anal. Chem.* **2007**, *79*, 8699–8704. [CrossRef] [PubMed]

93. Yang, H.; Luk, V.N.; Abeigawad, M.; Barbulovic-Nad, I.; Wheeler, A.R. A world-to-chip interface for digital microfluidics. *Anal. Chem.* **2009**, *81*, 1061–1067. [CrossRef] [PubMed]

94. Hatakeyama, T.; Chen, D.L.; Ismagilov, R.F. Microgram-scale testing of reaction conditions in solution using nanoliter plugs in microfluidics with detection by MALDI-MS. *J. Am. Chem. Soc.* **2006**, *128*, 2518–2519. [CrossRef] [PubMed]

95. Küster, S.K.; Fagerer, S.R.; Verboket, P.E.; Eyer, K.; Jefimovs, K.; Zenobi, R.; Dittrich, P.S. Interfacing droplet microfluidics with matrix-assisted laser desorption/ionization mass spectrometry: Label-free content analysis of single droplets. *Anal. Chem.* **2013**, *85*, 1285–1289. [CrossRef] [PubMed]

96. Fidalgo, L.M.; Whyte, G.; Ruotolo, B.T.; Benesch, J.L.; Stengel, F.; Abell, C.; Robinson, C.V.; Huck, W.T. Coupling microdroplet microreactors with mass spectrometry: Reading the contents of single droplets online. *Angew. Chem. Int. Ed.* **2009**, *48*, 3665–3668. [CrossRef] [PubMed]

97. Kelly, R.T.; Page, J.S.; Marginean, I.; Tang, K.; Smith, R.D. Dilution-free analysis from picoliter droplets by nano-electrospray ionization mass spectrometry. *Angew. Chem. Int. Ed.* **2009**, *48*, 6832–6835. [CrossRef] [PubMed]

98. Zhu, Y.; Fang, Q. Integrated droplet analysis system with electrospray ionization-mass spectrometry using a hydrophilic tongue-based droplet extraction interface. *Anal. Chem.* **2010**, *82*, 8361–8366. [CrossRef] [PubMed]

99. Li, Q.; Pei, J.; Song, P.; Kennedy, R.T. Fraction collection from capillary liquid chromatography and off-line electrospray ionization mass spectrometry using oil segmented flow. *Anal. Chem.* **2010**, *82*, 5260–5267. [CrossRef] [PubMed]

100. Pei, J.; Li, Q.; Kennedy, R.T. Rapid and label-free screening of enzyme inhibitors using segmented flow electrospray ionization mass spectrometry. *J. Am. Soc. Mass Spectrom.* **2010**, *21*, 1107–1113. [CrossRef] [PubMed]

101. Sun, S.W.; Slaney, T.R.; Kennedy, R.T. Label free screening of enzyme inhibitors at femtomole scale using segmented flow electrospray ionization mass spectrometry. *Anal. Chem.* **2012**, *84*, 5794–5800. [CrossRef] [PubMed]

102. Smith, C.A.; Li, X.; Mize, T.H.; Sharpe, T.D.; Graziani, E.I.; Abell, C.; Huck, W.T.S. Sensitive, high throughput detection of proteins in individual, surfactant-stabilized picoliter droplets using nanoelectrospray ionization mass spectrometry. *Anal. Chem.* **2013**, *85*, 3812–3816. [CrossRef] [PubMed]

103. Kautz, R.A.; Goetzinger, W.K.; Karger, B.L. High-throughput microcoil nmr of compound libraries using zero-dispersion segmented flow analysis. *J. Comb. Chem.* **2005**, *7*, 14–20. [CrossRef] [PubMed]

104. Lin, Y.Q.; Schiavo, S.; Orjala, J.; Vouros, P.; Kautz, R. Microscale LC-MS-NMR platform applied to the identification of active cyanobacterial metabolites. *Anal. Chem.* **2008**, *80*, 8045–8054. [CrossRef] [PubMed]

105. Kautz, R.; Wang, P.G.; Giese, R.W. Nuclear magnetic resonance at the picomole level of a DNA adduct. *Chem. Res. Toxicol.* **2013**, *26*, 1424–1429. [CrossRef] [PubMed]

106. Zheng, B.; Tice, J.D.; Roach, L.S.; Ismagilov, R.F. A droplet-based, composite PDMS/Glass capillary microfluidic system for evaluating protein crystallization conditions by microbatch and vapor-diffusion methods with on-chip x-ray diffraction. *Angew. Chem. Int. Ed.* **2004**, *43*, 2508–2511. [CrossRef] [PubMed]

107. Zheng, B.; Gerdts, C.J.; Ismagilov, R.F. Using nanoliter plugs in microfluidics to facilitate and understand protein crystallization. *Curr. Opin. Struct. Biol.* **2005**, *15*, 548–555. [CrossRef] [PubMed]

108. Stehle, R.; Goerigk, G.; Wallacher, D.; Ballauff, M.; Seiffert, S. Small-angle x-ray scattering in droplet-based microfluidics. *Lab Chip* **2013**, *13*, 1529–1537. [CrossRef] [PubMed]

109. Song, H.; Chen, D.L.; Ismagilov, R.F. Reactions in droplets in microfluidic channels. *Angew. Chem. Int. Ed.* **2006**, *45*, 7336–7356. [CrossRef] [PubMed]

110. Charwat, V.; Purtscher, M.; Tedde, S.F.; Hayden, O.; Ertl, P. Standardization of microfluidic cell cultures using integrated organic photodiodes and electrode arrays. *Lab Chip* **2013**, *13*, 785–797. [CrossRef] [PubMed]

111. Jansen-van Vuuren, R.D.; Armin, A.; Pandey, A.K.; Burn, P.L.; Meredith, P. Organic photodiodes: The future of full color detection and image sensing. *Adv. Mater.* **2016**, *28*, 4766–4802. [CrossRef] [PubMed]

112. Schutt, J.; Ibarlucea, B.; Illing, R.; Zorgiebel, F.; Pregl, S.; Nozaki, D.; Weber, W.M.; Mikolajick, T.; Baraban, L.; Cuniberti, G. Compact nanowire sensors probe microdroplets. *Nano Lett.* **2016**, *16*, 4991–5000. [CrossRef] [PubMed]

113. Fu, W.; Feng, L.; Panaitov, G.; Kireev, D.; Mayer, D.; Offenhausser, A.; Krause, H.J. Biosensing near the neutrality point of graphene. *Sci. Adv.* **2017**, *3*, e1701247. [CrossRef] [PubMed]

114. Schwierz, F. Graphene transistors. *Nat. Nanotechnol.* **2010**, *5*, 487–496. [CrossRef] [PubMed]